ELECTRIC ANALOG ANALYSIS OF THE GROUND-WATER SYSTEM IN CHAJ DOAB AREA, WEST PAKISTAN

by

Maqsood Ali Shah Gilani

A Thesis Submitted to the Faculty of the

DEPARTMENT OF HYDROLOGY

In Partial Fulfillment of the Requirements
For the Degree of

MASTER OF SCIENCE

In the Graduate College

THE UNIVERSITY OF ARIZONA

1964

STATEMENT BY AUTHOR

This thesis has been submitted in partial fulfillment of requirements for an advanced degree at the University of Arizona and is deposited in the University Library to be made available to borrowers under rules of the Library.

Brief quotations from this thesis are allowable without special permission, provided that accurate acknowledgment of source is made. Requests for permission for extended quotation from or reproduction of this manuscript in whole or in part may be granted by the head of the major department or the Dean of the Graduate College when in his judgment the proposed use of the material is in the interests of scholarship. In all other instances, however, permission must be obtained from the author.

SIGNED: Majoodhihed Gilani

APPROVAL BY THESIS DIRECTOR

This thesis has been approved on the date shown below:

John D. Ferris

J. G. FERRIS
Professor of Hydrology

May 1, 1964

Date

ELECTRIC ANALOG ANALYSIS OF THE GROUND-WATER SYSTEM IN CHAJ DOAB AREA, WEST PAKISTAN

by

Maqsood Ali Shah Gilani

ABSTRACT

The extensive canalization of the Doab, which was necessary to the development of irrigation agriculture induced added recharge to the ground-water system from the canal leakage. Disruption of the hydrologic balance of the regional flow system resulted in water-logging and soil salinization on a scale that threatens the entire economy of the region. The report establishes the cause-effect relationships involved and defines the functioning of the hydrologic system. Analog-simulation techniques for the analyses of ground-water systems in the Doab is developed. Analyses are made for (a) steady-state conditions that prevailed prior to the canal-irrigation period, and (b) non-steady state conditions for the canal-irrigation period from the year 1900 to 1960. The rise in ground-water levels, rate of infiltration from the main canals and their distributaries, net recharge rate to ground-water reservoir, and the effect of evapotranspiration on the rising ground-water levels are determined.

Recharge to ground-water from the rivers Jhelum and Chenab and discharge through evapotranspiration are found to be the main sources for maintaining hydraulic dynamic equilibrium during the pre-irrigation period. Further analysis indicates that, during the canal-irrigation period, the infiltration from the main canals and their distributaries is the cause of rise in ground-water levels. The net infiltration rate is of the order of 1767 million gallons per day and is a function of canal size. Out of this, 867 million gallons per day is the loss due to evapotranspiration, showing its importance in the ground-water system of the area.

Information resulting from this study provides a guide for more detailed study of the problem and establishes significant guidelines for future ground-water development in the Doab.

TABLE OF CONTENTS

LIST OF FIGURES

INTRODUCTION

Location and General Features of the Area

In the northern part of West Pakistan, a vast alluvial plain is traversed by the Indus River and its tributaries; the Jhelum, the Chenab, the Ravi, and the Sutlej Rivers. This alluvial plain, which consititutes part of the great Indus Basin, is subdivided into areas locally called the Doabs, meaning the land between two converging rivers. The name of the Doab is derived from the names of the rivers which bound it. For example, the Doab bounded on the north and west by the River Jhelum and on the south and east by the River Chenab, is the Chaj Doab.

In the northern part of West Pakistan (figure 1) the Chaj Doab comprises an area of 5,000 square miles of the Indus Plain. It is elongate in shape, about 170 miles long, and 40 miles wide, with the long axis trending southwest. The topographic slope is also to the southwest and ranges from more than 2 feet per mile in the northern part to less than a foot per mile on the south end with an average slope of the Doab of 1.5 feet per mile. The low relief of the plain and terrace is, however, broken by a few scattered bedrock hills known as Kiranas.

The principal cities are Gujrat, Sargodha, and Shahpur. All of the cities and most of the major towns are located on paved roads and are served by main lines or branch lines of the Pakistan Western Railway.

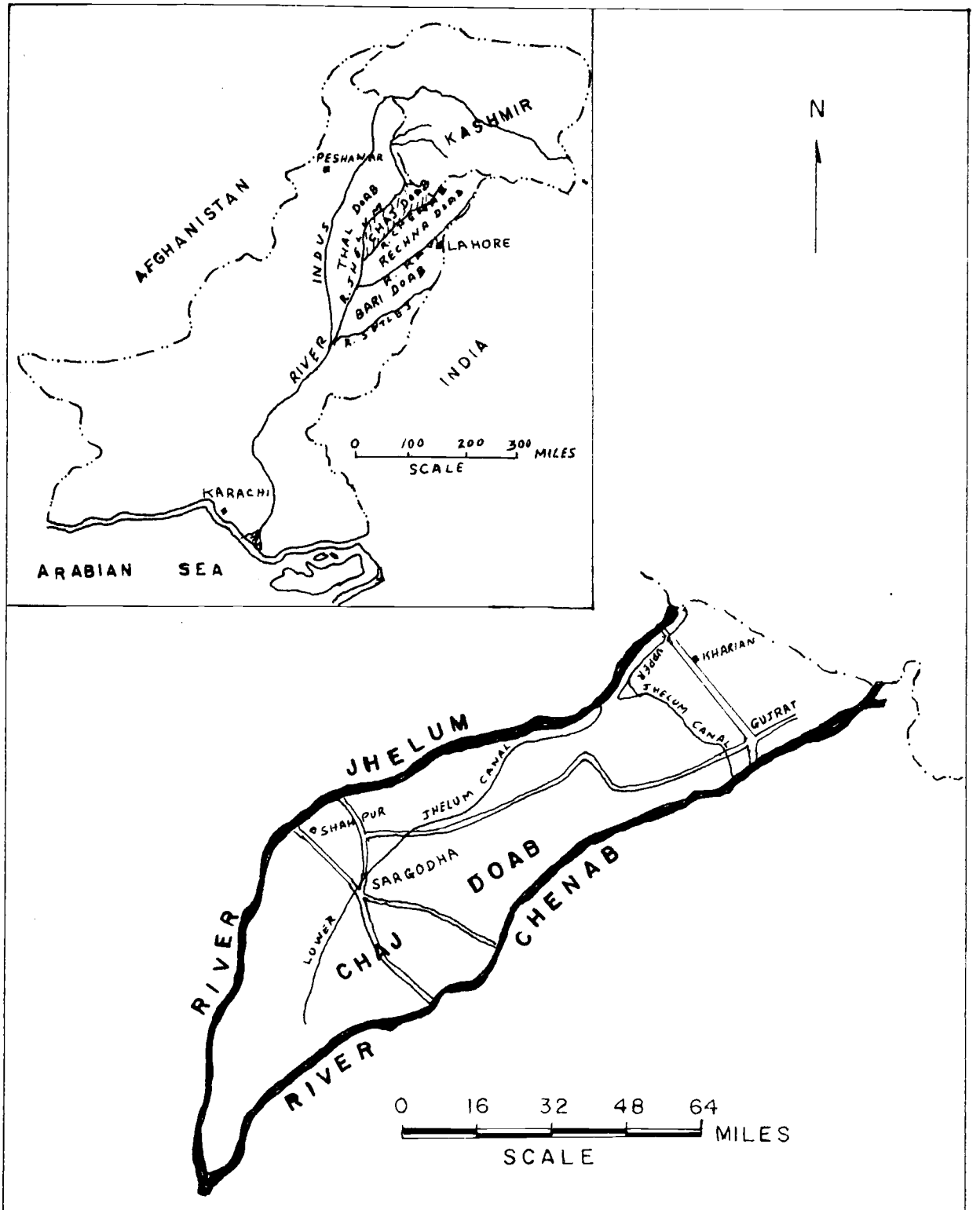

Figure 1. Index map of West Pakistan showing location of Chaj Doab

Agriculture is by far the major economic activity. There are two crop seasons in the areas - the "Kharif" and the "Rabi." The Kharif includes the monsoon season and extends from April 15 to October 15; during this season cotton, sugarcane, rice, and maize are grown. Rabi is the relatively dry winter season and extends from October 15 to April 15, during which wheat is the principal crop.

Rural population density is high, averaging about 500 persons per square mile and exceeding 800 persons per square mile in some areas.

Climate

The climate is typical of the low-lying interior of the Indo-Pakistan sub-continent and is characterized by large seasonal fluctuations in temperature and rainfall. The climate ranges from semihumid in the northeast to arid in the southwest. Daytime temperatures between the sixties and seventies and nighttime temperatures in the low forties are common from December to February. Frost is rare. Maximum temperatures of more than $105^{\circ}F$ are common from May to August, although the warmest months are May and June, prior to the monsoon rains.

Rainfall is generally scant and sporadic and, therefore, not a dependable source of crop moisture. Annual precipitation at different locations varies considerably over the period of observation. Mean annual precipitation at most stations of rain gauging for record periods of 1916 to 1957 is shown in figure 2. As shown in figure 2, the precipitation ranges from 22 to 27 inches per year in the upper reaches of the area in proximity to the Himalayan foothills to 10 inches per year and less in the southwest and lower half of the Chaj.

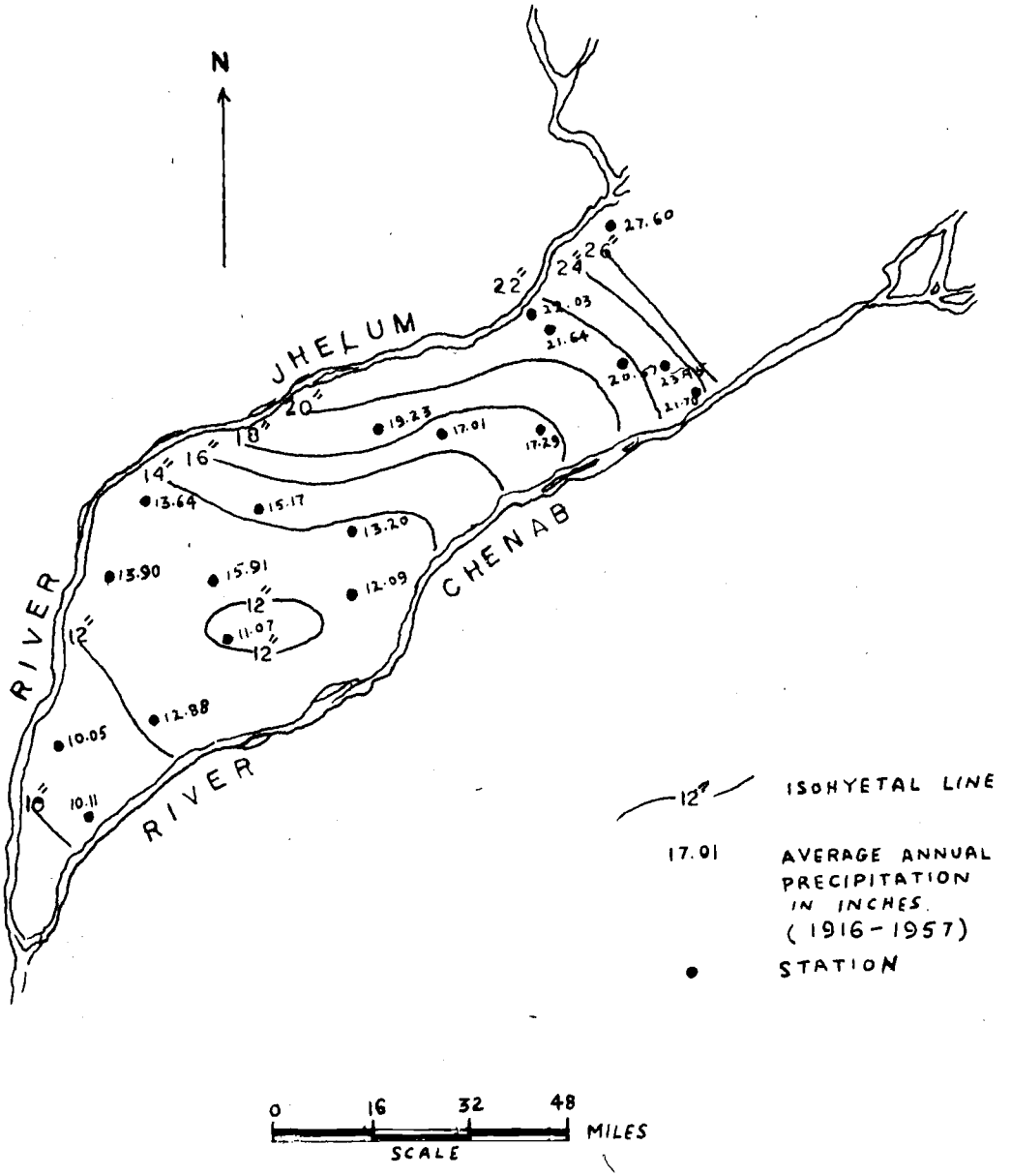

FIG. 2 ISOHYETAL MAP OF CHAJ DOAB

ADAPTED FROM SHEIKH & HUSSAIN.

Nature of Problem

West Pakistan is a region with precipitation so scanty that it is not a dependable source of crop moisture. The climate of the area makes irrigation a prerequisite to intensive agriculture. The favorable combination of other natural factors such as abundant surface water, flat terrain, and inherently fertile and well-drained soils makes irrigation possible. Throughout the recorded history of the land, man has endeavored to divert water to cultivate fields. Perennial and non-perennial canals have been built since the last century. The first perennial canal system in Chaj Doab started when the Lower Jhelum Canal opened in 1901, followed by the Upper Jhelum Canal in 1915, which also served as a link to transfer water from Jhelum River to Chenab River. These canal systems and their distributaries are part of other canal systems throughout the plain areas of West Pakistan. Accordingly, West Pakistan has one of the world's greatest irrigation developments.

Canal irrigation always involves diversion and redistribution of surface runoff and disruption of the hydrologic regimen is inevitable. Serious problems arise with the modification of the hydrologic environment. Permeable soils favor leakage from the canals and these losses deplete the supply available for irrigation. In addition, the seepage augments ground-water recharge which, under the flat hydraulic gradients that prevail in the area, can not be discharged through subsurface drainage. Since the beginning of canal irrigation, the ground-water levels in the Doabs have risen and stabilized eventually at depths below land surface ranging from 5 to 20 feet. Consequently, water-logging and increasing

soil salinity has resulted. Water-logging and soil salinity remove once fertile land from agriculture. The province of West Pakistan is faced with national disaster unless the twin menace of water-logging and soil salinity is alleviated. Figure 3 shows a typical view of main canals in Chaj Doab. In figure 4 and 5, the effects of water-logging and soil salinity resulting in deterioration of agricultural land is exhibited.

Previous Investigations

Since 1915, when salinity and water-logging became major problems, the observation-well data from the various Doabs have been a subject of continuing study by scientists from several government agencies and universities. Most of the studies were of such limited nature that the findings were generally inconclusive and often misleading. The cause had been related to various factors such as monsoon rains, local recharge to the water table, induced by rice and cotton irrigation, or bedrock beneath the alluvium interfering with ground-water movement. Midha, Luthra and Vaidhianathan (1937) showed that canal seepage losses must be an important increment of ground-water recharge. The first comprehensive study of the problem of subsurface drainage was made by Carlston (1953). His evaluation of the available hydrologic and geologic data for Rechna Doab (an adjacent area to Chaj Doab) indicated that canal leakage was the major factor involved.

Fig. 3.--A Typical Canal View in Chaj Doab, West Pakistan

Fig. 4 & 5.--The Lands Deteriorated by Water-logging and Soil Salinity. White Surfaces Show the Accumulation of Salts Brought to Land Surface by the Rise of Ground-Water Levels with Attendant Evaporation.

In 1954, the Government of the Punjab (later integrated into one provincial Government of West Pakistan) and the United States International Cooperation Administration (afterwards known as Agency for International Development - AID) began a series of joint investigations of the hydrology, geology, and soils of the Doab areas of West Pakistan. These investigations were started by the Irrigation Branch of the Punjab Government and since 1960, have been taken over by the Water and Soils Investigation Division (WASID) of the West Pakistan Water and Power Development Authority (WAPDA). The objectives of the investigations are to make an inventory of the water and soils resources of the areas of West Pakistan and to describe the relationships between irrigation activities and natural hydrologic factors as they pertain to waterlogging and subsurface drainage problems. A recent analysis of the problem by Greenman, Swarzenski, and Bennett (1963) indicates that leakage from the existing canal distribution system is the principal cause of subsurface-drainage problems in the Punjab, and it also is the major component of ground-water recharge.

The author has used most of the basic data compiled and produced by WASID for the present work.

Purpose and Method of Present Study

Lowering the water table in the Doabs in order to apply more water to reclaim salinized land by leaching down the surface salts involves a complicated water-management problem, because many variables and boundary limitations affect the ground-water system in the area.

The problem cannot be solved by ordinary ground-water mathematical methods. The use of electric-analog models, however, can be applied to solve the problem if the boundary conditions and related factors are formulated.

It is the aim of present study to formulate the historical rise in ground-water levels over a period of sixty years, i.e. 1900-1960, using the electric-analog model of Chaj Doab area constructed by the United States Geological Survey Analog Model Unit in Phoenix, Arizona. The study included the following hydrologic settings:

1. Steady-state conditions that prevailed prior to canal-irrigation systems and an evaluation of evapotranspiration rates.
2. Non-steady state conditions; analog simulation of recharge from the various canals was established with the addition of canal systems to the electrical model. Rise of ground-water levels with time, the rate of infiltration from the main canals and their distributaries and the net accretion rate to the ground-water reservoir, and evapotranspiration effects were determined.

The study was made using the available water-level data, the geology and aquifer constants (transmissibility and specific yield as determined through pumping tests by WASID) and certain assumptions relating to boundary conditions.

Acknowledgments

The author is indebted to Dr. John W. Harshbarger, Chairman of the Hydrology Committee, and Mr. John G. Ferris, thesis director, for their continuous encouragement and helpful discussions without which this work would have been impossible. The author is also obliged to Mr. Eugene P. Patten in charge of the Analog Model Unit, United States Geological Survey at Phoenix, Arizona for his guidance in conducting the experiment and for the facilities to carry out this work in his laboratory. All the members of his staff at the laboratory were most cooperative.

The author is also grateful to the Water and Soils Investigation Division of West Pakistan Water and Power Development Authority, and the United States Agency for International Development for providing the opportunity and facilities for training the author in hydrology at the University of Arizona.

The author is thankful to his mother and wife who have been a source of constant inspiration from a distance of more than 13,000 miles during the author's long stay in the United States.

GROUND-WATER GEOLOGY

The investigations conducted by the Water and Soils Investigation Division of Water and Power Development Authority, West Pakistan, included detailed studies of the physiography and geology of Chaj Doab. More than two hundred exploratory holes were drilled to ascertain the subsurface lithology of the Doab. The physiographic and geologic units of the area were described by Kidwai (1962). A brief summary is given here.

Physiographic Units

Chaj Doab may be divided into the following physiographic units which are shown in figure 6.

Kirana Hills

The Kirana Hills, a group of bedrock hills rising abruptly in the southern part of Chaj Doab are as much as 1000 feet above the surrounding plains. These outcrops show a northwesterly alignment, which expresses the existence of a bedrock ridge known as Shahpur-Delhi Ridge (Pre-Cambrian rocks) that is largely buried by alluvium. The Kirana Hills are a prominent but minor feature in the vast alluvial complex covering the area.

Pabbi Hills

The Pabbi Hills, which occupy a small area in the northernmost part of Chaj Doab, rise 400 to 500 feet above the surrounding alluvial and piedmont deposits. These hills, formed by an anticline of rocks

of the Siwalik system, are part of the Himalayan foothills. Widespread development of gullies and vertical erosion of both the Siwaliks and overlying loess deposits have imparted a typical badland topography to the area, particularly on the northern flank of the anticline.

Piedmont Area

This area is located in the northeastern part of Chaj Doab near the Jammu and Kashmir boundary. The Piedmont area is transitional between the alluvial plain and the Himalayan foothills and is composed largely of alluvial fans dissected by hill torrents and small perennial streams.

Alluvial Plain

Nearly the entire area of Chaj Doab lies within the Punjab Plains, a part of the Indo-Gangetic Alluvial Plain. The alluvium of the area consists of sand and silt with lesser amount of clay and gravel that have been deposited by present and past tributaries of the Indus River. The mode of deposition by large, constantly shifting rivers, resulted in heterogeneous formations. The individual strata have limited horizontal and vertical continuity. The following three subdivisions are based on the present relationship of the surface features and the rivers.

1. Abandoned Flood Plain: This area is several feet higher than the active flood plain. Paralleling the present river in a belt as much as 20 miles wide, it represents flood plains that have been abandoned in comparatively recent times by the present rivers. The deposits of the abandoned flood plains are similar

to those found in the active flood plain. Common features are channel scars, oxbow lakes, and levees.

2. Active Flood Plain: This subdivision includes the meander belt and present flood plain of the rivers Jhelum and Chenab. It contains natural levees - a few inches to about 5 feet high - back-water swamps, meander scars, and the sand bars.

3. Bar Uplands: Bar uplands are largely interfluvial areas composed of relatively older alluvium. Because of their large areal extent and elevation above bordering flood plains, these interfluves, termed as bar uplands, are the most significant physiographic feature. Typically, the bar uplands rise abruptly from the flood plains and are bordered by steep scarps 5 to 25 feet high. At some places, however, the boundary is not distinct.

Geologic Units

In the Punjab Plains, including Chaj Doab, Quaternary alluvium has been deposited on semi-consolidated Tertiary rocks or on a basement of metamorphic and igneous rocks of Pre-Cambrian age (Kiranas). In Chaj Doab, the Tertiary rocks in the Pabbi Hills area in northeast are found in the exposed Siwalik system. In the area of buried bedrock ridge, exploratory drilling has revealed that the Pre-Cambrian-basement rocks are overlain directly by Quaternary alluvium. To the northeast and southwest of the bedrock ridge, test holes drilled to a maximum depth of 1500 feet bottom in alluvium. Therefore, no information is available regarding the total thickness of the alluvium deposits. An

illustration (figure 7) shows the contours of depth to bedrock as revealed through exploratory drilling.

Three geologic units of subordinate regional significance are namely; the Potwar Loess, Piedmont Deposits, and Aeolian Deposits. The occurrence of the Potwar Loess is restricted to the northern part of the Pabbi Hills. Piedmont Deposits are confined to a narrow belt, generally less than 15 miles wide and adjacent to the Himalayan foothills. Both formations lay beyond the area of the model study. Scattered sand dunes in the southern part of Chaj Doab represent the Aeolian Deposits which cover very small areas or fill local depressions. These deposits are intimately associated with the alluvium and their separation, therefore, are generally not practical.

The principal ground-water reservoir of the Chaj Doab area is the alluvium. Essentially, all of the Chaj Doab area under the present study is comprised of alluvial complex underlain in the south-central part by the buried bedrock ridge of Pre-Cambrian age. These two formations, therefore, merit further attention and discussion.

Alluvial Complex and Its Water-Bearing Characteristics

The alluvium of Chaj Doab was derived from the mountain ranges to the north and deposited in a subsiding trough by the present and former tributaries of the Indus River. The alluvial complex is of Pleistocene and Recent age, and consists of unconsolidated fine to medium sand, silt and clay. Beds of gravel and very coarse sand are uncommon. However, granules of siltstone or mudstone may be found embedded in silty or clayey sand in many places. Also associated with the fine-grained strata are

kankar, a calcium carbonate deposit of secondary origin. The study of drill cuttings and electric logs show that the clay zones within the alluvium are relatively thin and are not areally extensive. With the exception of local clay lenses, a few feet thick, the fine-grained portions of the alluvium generally consists of sandy, gravelly, or silty clay. The lithology of the alluvium as inferred from the study of well samples and electric logs is shown in figure 8. The illustration shows the heterogeneous character of the uppermost 600 feet of the alluvium in downstream and transverse directions, and the random distribution of clay zones within the alluvium. Local accumulations of relatively fine-grained material are found in the upper part of the Doab and in the vicinity of the bedrock ridge.

The alluvial deposits notwithstanding their heterogeneous composition, form a unified, highly transmissive aquifer, in which ground water occurs essentially under water-table conditions. Over the area, tube wells yield 900 to 1800 gallons per minute. The uppermost 300 feet of the aquifer is the most productive zone. The average vertical permeability has been reported to be considerably less than the average lateral permeability throughout most of the area (Bennett and others, 1964).

Bedrock Ridge

The bedrock hills known as Kiranas are the peaks of a buried ridge which underlies the south-central portion of Chaj Doab. It has also been referred to as the Shahpur-Delhi Ridge, from the inference

Fig. 8.--Panel Diagram Showing Sub-Surface Geology of Chaj Doab


SEA LEVEL
SEA LEVEL
EXPLANATION
CLAY
SILT
SAND
BEDROCK

that it represents the northwesterly extension of the ancient Aravalli Mountain system in India. Available data shows that the average thickness of the alluvium over the crest of the ridge is of the order of 400 to 500 feet. (Greenman, Swarzenski and Bennett, 1963). The influence of the buried ridge on the movement of ground water has been the subject of much discussion and the estimates of its effects have been reported from negligible to that of a total barrier. However, according to a recent report by Greenman and others, it has been inferred that the blocking and damming effect of the bedrock outcrops on the regional movement of ground water are probably negligible, as only a very small part of the total area is occupied by the bedrock hills. Though the alluvium is considerably thinner over the ridge, the average elevation of the ridge is not sufficiently great to affect significantly the movement of water in the upper several hundred feet of the alluvium where the bulk of ground-water flow takes place.

ELECTRICAL ANALOGY OF GROUND-WATER FLOW

General Discussion

Ideally, the solution of a field problem seeks to determine the cause-effect relationship for a specified system. A satisfying form of solution would be a complete mathematical description, and many refined techniques have been developed for the analytical treatment of field problems. However, analytic formulations are possible only for boundary problems of simple geometry. The analog method provides a powerful tool for analysis of very complex boundary-value problems and clarifies the physical interpretation.

Two systems are said to be analogous if there is complete correspondence between related elements of the two systems and cause-effect relation of these elements to the system as a whole. In other words, two systems are analogous if their response to similar input stress is similar in form. Excitation (cause) and response (effect) values are expressed generally in terms of variables dependent upon time and position within the field.

The Analogy

The application of electric analogs for simulating geologic and hydrologic conditions is based on the correspondence between the basic laws of electrical and laminar liquid flow.

If Q is the rate at which water flows through an aquifer of transmissibility, T; if the flows occur through an aquifer cross section of width, L; and if the hydraulic gradient (head loss per unit length of flow path), I; the relation between these terms may be written according to Darcy's Law as

$$Q = TIL \tag{3.1}$$

In analogous way, if i is the density of electric current flowing through a conductive sheet of resistance R, and if V is the electric potential drop across the sheet, then according to Ohm's Law, we have

$$i = \frac{V}{R} \tag{3.2}$$

The analogy between the two flow systems given in equation 3.1 and 3.2 allows proportional comparison of terms i, V and $\frac{1}{R}$ with physically similar terms $\frac{Q}{L}$, I and T. Consideration of the appropriate differential equations for the flow of ground water and electricity provide the basis for a more complete understanding of the analogous relationship. If more than two variables are present, the description will be in terms of partial-differential equations. These equations describe the internal state of physical systems being studied with regard to the pertinent forces involved.

Equations of Ground Water and Their Electrical Equivalence

Ground-water systems, being dissipative, have equations of motion which specify the dissipation of the energy due to the motion

of the liquid. The differential equations representing the system must state for each infinitesimal volume of the aquifer that the energy dissipative rate is equal to the rate of change of stored energy and the rate of change of energy entering from points external to the infinitesimal volume. The differential equation representing this is:

$$P \nabla^2 h = S \frac{\partial h}{\partial t} + W(x, y, z, t) \tag{3.3}$$

in which

$$\nabla^2 h = \frac{\partial^2 h}{\partial x^2} + \frac{\partial^2 h}{\partial y^2} + \frac{\partial^2 h}{\partial z^2}$$

P = Energy dissipative rate constant or permeability.

h = The function representing the liquid pressure at the point or hydraulic head.

$\frac{\partial h}{\partial t}$ = The rate of change of the hydraulic head.

S = Coefficient relating the release of energy with a given change in head.

$W(x, y, z, t)$ = The rate at which energy enters the boundary of the region other than due to the hydraulic gradient head as a function of time.

Equation 3.3 can be described for various conditions.

Laplace Equation

If the internal points of ground-water flow systems do not have changes in head as a function of time and do not have recharges from regions external to the system, equation 3.3 reduces to the Laplace Equation, i.e.

$$\nabla^2 h = 0 \tag{3.4}$$

Poisson Equation

When the function W (x, y, z, t) in equation 3.3 is independent of time and the hydraulic heads throughout the system become independent of time, equation 3.3 becomes Poisson's Equation of the following form:

$$\nabla^2 h = \frac{W}{P}(x, y, z) \tag{3.5}$$

Diffusion Equation

The ground-water flow system, having no recharge from points external to the system but having the hydraulic head changing as a function of time, will yield equation 3.3 into the form:

$$\nabla^2 h = \frac{S}{P}\frac{\partial h}{\partial t} \tag{3.6}$$

which is called the Diffusion Equation and is the non-equilibrium equation in studies on ground-water flow. This equation was first related to ground-water problems by C. V. Theis (1935).

If the ground-water flow is such that it can be described by two space coordinates only, then the above equations reduce to the following by letting $\frac{\partial^2 h}{\partial z^2} = 0$, and $W(x, y, z, t) = W(x, y, t)$.

Then we have:

$$P\left(\frac{\partial^2 h}{\partial x^2} + \frac{\partial^2 h}{\partial y^2}\right) = S\frac{\partial h}{\partial t} + W(x, y, t) \tag{3.3a}$$

$$\frac{\partial^2 h}{\partial x^2} + \frac{\partial^2 h}{\partial y^2} = 0 \tag{3.4a}$$

$$\frac{\partial^2 h}{\partial x^2} + \frac{\partial^2 h}{\partial y^2} = \frac{W}{P}(x, y) \tag{3.5a}$$

and

$$\frac{\partial^2 h}{\partial x^2} + \frac{\partial^2 h}{\partial y^2} = \frac{S}{P} \frac{\partial h}{\partial t} \qquad (3.6a)$$

The analogy to be exploited by the analog computer is that existing between the flow of fluids and the flow of electricity. Two equations that describe diffusion of hydraulic and electrical energy when inertia and inductance are neglected are given by Jacob (1950) and Karplus (1958) as equations 3.7 and 3.8 respectively as follows:

$$\nabla^2 h = \frac{S}{T} \frac{\partial h}{\partial t} \qquad (3.7)$$

and

$$\nabla^2 V = \rho \frac{C}{V_o} \frac{\partial V}{\partial t} \qquad (3.8)$$

where h is the head in the aquifer above an arbitrary horizontal reference plane.

T is the coefficient of transmissibility (permeability times thickness of aquifer).

ρ is the specific resistance of the analog matrix in the direction of flow.

$\frac{C}{V_o}$ is the electrical capacity of the analog matrix per unit volume of reservoir or analog matrix.

V is the voltage at some point (x, y, z) in the analog.

V_o is (∇x. ∇y. ∇z) of reservoir or analog matrix.

∇^2 is the operator $\left(\frac{\partial^2}{\partial x^2} + \frac{\partial^2}{\partial y^2} + \frac{\partial^2}{\partial z^2} \right)$

The above equations (3.7 and 3.8) are analogous as may be seen by substituting into the following expressions from Theis's Equation (1938) and Darcy's Law as well as their electrical equivalents, Coulomb's Law and Ohm's Law, and expressing the space variables as discrete quantities. From Theis's Equation

$$S = \frac{Q_w}{\Delta h \, \Delta x \, \Delta y} \tag{3.9}$$

and from Darcy's Law, assuming flow in the x direction only,

$$T = \frac{q_w}{\Delta y \frac{\Delta h}{\Delta x}} \tag{3.10}$$

Also from Coulomb's Law,

$$C = \frac{Q_E}{\Delta V} \tag{3.11}$$

and from Ohm's Law, assuming flow in the x direction only,

$$\rho = \frac{R \, \Delta y \, \Delta z}{\Delta x} = \frac{\Delta V \, \Delta y \, \Delta z}{\Delta x \, q_E} \tag{3.12}$$

where

ρ is resistivity of the conductor.

Q_w is the quantity of water.

Q_E is the quantity of electricity.

q_w is the rate of flow of water.

q_E is the rate of flow of electricity.

R is resistance of uniform conductor of length Δx and cross-sectional area $\Delta y \, \Delta z$.

Substituting the various terms, the equations 3.7 and 3.8 become:

$$\nabla_x^2 h = \frac{Q_w}{q_w \Delta x^2} \frac{\partial h}{\partial t_w} \tag{3.13}$$

and

$$\nabla_x^2 V = \frac{Q_E}{q_E \Delta x^2} \frac{\partial V}{\partial t_E} \tag{3.14}$$

From these two equations, it is found that both systems are similar.

Finite Difference Network

The distinctive feature of potential fields is that the system parameters are distributed in a continuous manner throughout space and the specification of the dependent variable (potential function or stream function) requires the specification of the location of the point under consideration within the system. In potential-field problems, therefore, the space variables x, y, z as well as the time variable t are continuously independent variables, and the equations governing the system are partial-differential equations. The finite-difference approach involves the replacement of the distributed system by an assemblage of lumped elements in such a manner that the characteristics of the original field are approximately conserved. This is permissible and useful provided that the mesh is made fine or in other words, the space between adjacent nodes is sufficiently small. Finite-difference approximation of a partial-differential equation is made by superimposing a discrete coordinate grid upon the field, and attention is then limited to the node points of this grid. Approximations for

the first and second derivatives in terms of the node potentials are then obtained. The development of finite-difference equations for the expression $\nabla^2 h$ is the basis for the use of relaxation methods and it is necessary to determine the finite-difference equations for the expression $\nabla^2 h = 0$; i.e., the Laplace Equation.

Laplace Equation

Consider the following three figures for one-, two-, and three-dimensional fields with finite-difference grid and typical nodes:

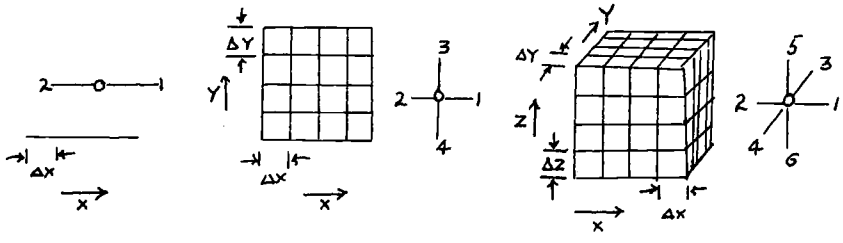

(a) (b) (c)

Consider first the one-dimensional field as shown in figure a. If the hydraulic heads h_1, h_o, and h_2 are assumed to exist at net points, respectively, the average hydraulic gradient between nodes 1 and 0 may be expresses as their head difference divided by the distance between them:

$$\left(\frac{dh}{dx}\right)_{0-1} \cong \frac{h_1 - h_0}{\Delta x} \tag{3.15}$$

In a similar way, the average gradient between nodes 2 and 0 is

$$\left(\frac{dh}{dx}\right)_{2-0} \cong \frac{h_0 - h_2}{\Delta x} \tag{3.16}$$

In these expressions, it is assumed that the hydraulic gradient is constant between adjacent nodes. Expression 3.15 is termed as a "forward-difference" approximation. $\left(\frac{\partial h}{\partial x}\right)_{0-1}$ may be considered to represent the hydraulic gradient midway between nodes 0 and 1. Similarly, $\left(\frac{\partial h}{\partial x}\right)_{2-0}$ represents $\frac{\partial h}{\partial x}$ midway between 2 and 0. The second derivative is the rate of change of the first derivative.

$$\left(\frac{d^2h}{dx^2}\right)_0 \cong \frac{(dh/dx)_{0-1} - (dh/dx)_{2-0}}{\Delta x} \tag{3.17}$$

or

$$\begin{aligned}\left(\frac{d^2h}{dx^2}\right)_0 &\cong \frac{1}{\Delta x}\left[\frac{h_1 - h_0}{\Delta x} - \frac{h_0 - h_2}{\Delta x}\right] \\ &\cong \frac{1}{\Delta x^2}\left[h_1 + h_2 - 2h_0\right]\end{aligned} \tag{3.18}$$

Equation 3.18 is a finite-difference approximation of $\nabla^2 h$ in one-space dimension.

In the two-dimensional field illustrated in figure b, above, average values for the first space dimensions at points midway between node 0 and the four adjacent nodes are approximated as

$$\left(\frac{\partial h}{\partial x}\right)_{0-1} \cong \frac{h_1 - h_0}{\Delta x} \qquad \left(\frac{\partial h}{\partial y}\right)_{0-3} \cong \frac{h_3 - h_0}{\Delta y}$$

and (3.19)

$$\left(\frac{\partial h}{\partial x}\right)_{2-0} \cong \frac{h_0 - h_2}{\Delta x} \qquad \left(\frac{\partial h}{\partial y}\right)_{4-0} \cong \frac{h_0 - h_4}{\Delta y}$$

and the second derivatives are

$$\left(\frac{\partial^2 h}{\partial x^2}\right)_0 \cong \frac{1}{\Delta x^2}\,(h_1 + h_2 - 2h_0)$$

$$\left(\frac{\partial^2 h}{\partial y^2}\right)_0 \cong \frac{1}{\Delta y^2}\,(h_3 + h_4 - 2h_0) \qquad (3.20)$$

The Laplacian in two dimensions then becomes,

$$\nabla^2 h = \frac{\partial^2 h}{\partial x^2} + \frac{\partial^2 h}{\partial y^2} \cong \frac{1}{\Delta x^2}\,(h_1 + h_2 - 2h_0) + \frac{1}{\Delta y^2}\,(h_3 + h_4 - 2h_0) \qquad (3.21)$$

and if $\Delta x = \Delta y$, equation 3.21 reduces to

$$\nabla^2 h \cong \frac{1}{\Delta x^2}\,[\,h_1 + h_2 + h_3 + h_4 - 4h_0\,] \qquad (3.22)$$

and the Laplace Equation will be

$$h_1 + h_2 + h_3 + h_4 - 4h_0 \cong 0 \qquad (3.23)$$

Similarly, for three-space coordinates, we get

$$\left(\frac{\partial h}{\partial x}\right)_{0\text{-}1} \cong \frac{h_1 - h_0}{\Delta x} \qquad \left(\frac{\partial h}{\partial y}\right)_{0\text{-}3} \cong \frac{h_3 - h_0}{\Delta y}$$

$$\left(\frac{\partial h}{\partial x}\right)_{2\text{-}0} \cong \frac{h_0 - h_2}{\Delta x} \qquad \left(\frac{\partial h}{\partial y}\right)_{4\text{-}0} \cong \frac{h_0 - h_4}{\Delta y}$$

and (3.24)

$$\left(\frac{\partial h}{\partial z}\right)_{0\text{-}5} \cong \frac{h_5 - h_0}{\Delta z} \qquad \left(\frac{\partial h}{\partial z}\right)_{6\text{-}0} \cong \frac{h_0 - h_6}{\Delta z}$$

where the subscripts refer to the nodes identified in figure c above. Then the second derivatives are obtained as before,

$$\left(\frac{\partial^2 h}{\partial x^2}\right)_0 \cong \frac{1}{\Delta x^2}\,(h_1 + h_2 - 2h_0)$$

$$\left(\frac{\partial^2 h}{\partial y^2}\right)_0 \cong \frac{1}{\Delta y^2}\,(h_3 + h_4 - 2h_0)$$

and (3.25)

$$\left(\frac{\partial^2 h}{\partial z^2}\right)_0 \cong \frac{1}{\Delta z^2}\,(h_5 + h_6 - 2h_0)$$

and when combined,

$$\nabla^2 h \cong \frac{1}{\Delta x^2}\,(h_1 + h_2 - 2h_0) + \frac{1}{\Delta y^2}\,(h_3 + h_4 - 2h_0) + \frac{1}{\Delta z^2}\,(h_5 + h_6 - 2h_0) \qquad (3.26)$$

and if $\Delta x = \Delta y = \Delta z$, this expression reduces to

$$\nabla^2 h \cong \frac{1}{\Delta x^2}\,[\,h_1 + h_2 + h_3 + h_4 + h_5 + h_6 - 6h_0\,]$$

and for Laplace's Equation, we get

$$h_1 + h_2 + h_3 + h_4 + h_5 + h_6 - 6h_0 \cong 0 \qquad (3.27)$$

Equations 3.23 and 3.27 indicate that, if an uniform net spacing is chosen in all directions, the hydraulic heads at any node of a field governed by Laplace's Equation may be found by averaging the heads existing at all adjacent nodes.

Similar conditions occur for electric models. Consider now the node formed in an electric circuit by the junction of two resistors as shown in this figure.

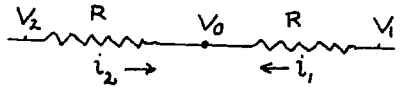

According to Kirchhoff's current law,

$$i_1 + i_2 = 0 \tag{3.28}$$

or

$$\frac{V_1 - V_0}{R} + \frac{V_2 - V_0}{R} = 0$$

or

$$\frac{1}{R} \left[V_1 + V_2 - 2V_0 \right] = 0 \tag{3.29}$$

Comparison of equations 3.18 and 3.29 reveals that the typical node of the above figure is analogous to a typical node of the finite grid, if R is made proportional to (Δx^2). The voltage at node 0 is proportional to h_0.

Similarly for two-dimensional systems of Laplace's Equations, the relation between voltage may be determined by summing the current at a node. If a point 0 and its four nearest neighbors are connected by four resistors R as in this figure,

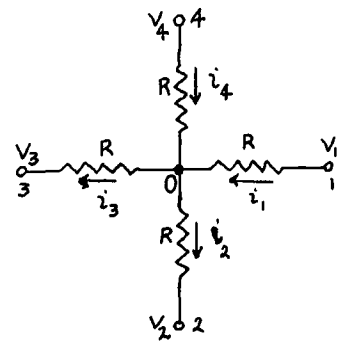

the current flowing through the resistors, and the sum of the currents are given in terms of voltages as:

$$i_1 - i_2 - i_3 + i_4 = 0$$

or

$$\frac{V_1 - V_0}{R} - \frac{V_0 - V_2}{R} - \frac{V_0 - V_3}{R} + \frac{V_4 - V_0}{R} = 0 \qquad (3.30)$$

from which we get,

$$(V_1 + V_2 + V_3 + V_4 - 4V_0) = 0 \qquad (3.31)$$

The analogy between equations 3.23 and 3.31 is evident. Similarly, for three-dimensional systems, we have

$$V_1 + V_2 + V_3 + V_4 + V_5 + V_6 - 6V_0 = 0 \qquad (3.23)$$

Since the Laplace Equation is linear, the interior voltage values will bear the same ratio to the interior values of h as the boundary voltage to the boundary values of h.

Poisson Equation

A similar treatment for Poisson's Equation is done as that of Laplace's Equation. In ground-water flow, the Poisson Equation for two-dimensional flow in finite-difference approximation reduces to

$$\frac{h_1 + h_2 + h_3 + h_4 - 4h_0}{L^2} = \frac{W}{T} \quad (x_0, y_0) \tag{3.33}$$

where

$$L = \Delta x = \Delta y.$$

For an equivalent electric circuit, we will have a current i being drained from node 0. Therefore, for Poisson's Equation, we get

$$\frac{V_1 + V_2 + V_3 + V_4 - 4V_0}{R} = i \tag{3.34}$$

A typical node of this circuit is as shown in this figure.

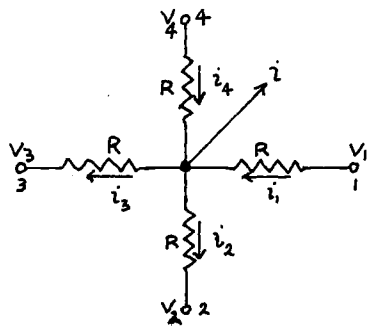

Consequently, for the analogy to hold between the numerical results required in equation 3.33 and the electric voltage obtained in equation 3.34, we see that

$$Ri = L^2 \frac{W}{T} (x_0, y_0)$$

or

$$i = \frac{L^2}{R} \cdot \frac{W}{T} (x_0, y_0) \tag{3.35}$$

Diffusion Equation

The Diffusion Equation for two-dimensional ground-water flow systems in the finite-difference form is as follows:

$$\frac{h_1 - h_0}{L^2} + \frac{h_2 - h_0}{L^2} + \frac{h_3 - h_0}{L^2} + \frac{h_4 - h_0}{L^2} = \frac{S}{T} \frac{\partial h_0}{\partial t} \tag{3.36}$$

or

$$\frac{h_1 + h_2 + h_3 + h_4 - 4h_0}{L^2} = \frac{S}{T} \frac{\partial h_0}{\partial t} \tag{3.37}$$

where subscripts 1, 2, 3, 4 have usual meaning representing adjacent nodes in the x and y direction. Just as in the simulation of Laplace's Equation, the terms on the left side of equation 3.36 represent current flow through resistors of magnitude L^2. The term on the right side of the equation must, therefore, also be represented by current. This is accomplished by connecting a capacitor of magnitude $\frac{S}{T}$ from each network "node to ground." Typical nodes of the network-analog circuit for the equation 3.36 is shown here.

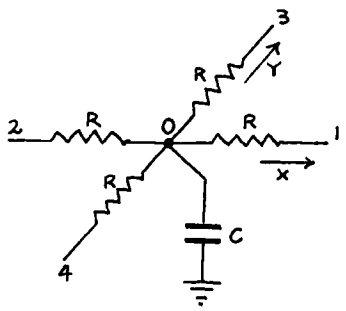

Kirchhoff's current law then specified for two-dimensional case is

$$\frac{V_1 - V_0}{R} + \frac{V_2 - V_0}{R} + \frac{V_3 - V_0}{R} + \frac{V_4 - V_0}{R} = \frac{\partial V_0}{\partial t} \qquad (3.39)$$

The formulation of hydrologic problems governed by the Diffusion Equation demands the specification of boundary conditions as well as initial conditions. The boundary conditions are, in general, similar to those specified for Laplace's Equation and may include equipotential boundaries, streamline boundaries and boundaries for which the normal derivative of the potential function is specified. In addition, the magnitude of the potential function at all points within the field must be specified for some time, usually at $t = 0$.

ELECTRIC ANALOG ANALYSIS OF THE PROBLEM

The ground-water reservoir underlying the area is an unexploited resource of economic value. It is recognized that the scientific management of the ground-water reservoir is the key to permanent irrigation agriculture in West Pakistan. West Pakistan's Water and Power Development Authority (WAPDA) has prepared a long-range program for reclaiming the irrigated lands of the Doab areas. The essential feature of this program is a proposed network of tube wells, located with an average density of about one per square mile. Ground-water withdrawals will serve the dual purpose of helping to supply irrigation requirements, and providing subsurface drainage. Notwithstanding the feasibility and inherent advantages of tube well reclamation methods, it is inevitable that just as the superposition of canal systems on the native environment caused considerable side effects, large scale ground-water withdrawals again will disturb the hydrologic regimen. The effect of evaporation under heavy pumping will be an important factor controlling the ground-water potential. As an illustration, hydrographs from two wells in Chaj Doab (figure 9) show the effect of direct evaporation from the water table. These hydrographs show the rise of once deep water tables by the introduction of canal irrigation. After the year 1901 when the canal system was introduced, the water table rose distinctly almost as a straight line on the hydrographs, until it was only 8 to 10 feet below land surface. At this point, vapor discharge to the atmosphere is evidenced by the rapid fluctuations in the water table and also by

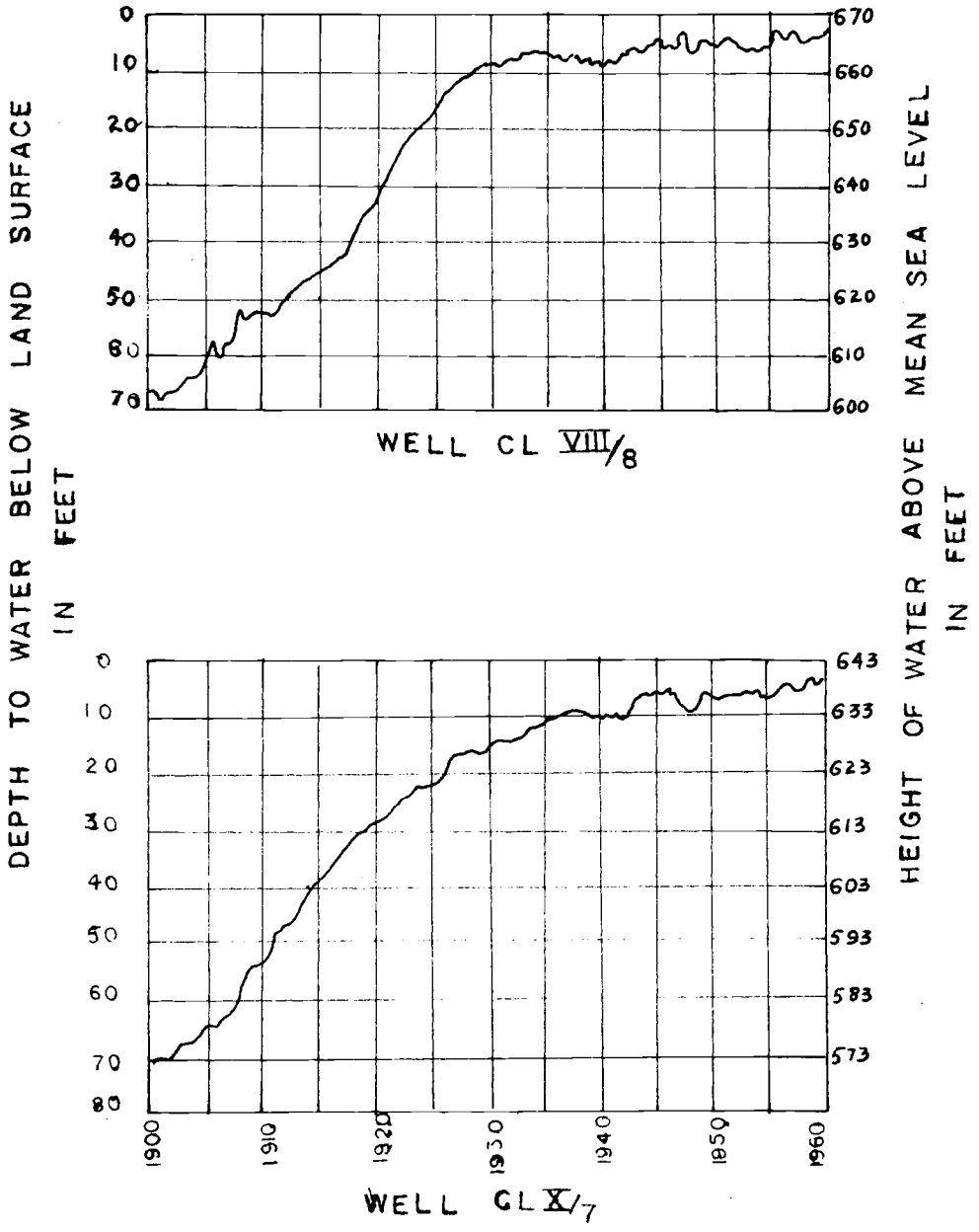

FIG.9 HYDROGRAPHS OF WATER TABLE RISE IN CHAJ DOAB

the sharp break in slope mark, the point at which vapor discharge by evaporation removed the imposed recharge input and the water table stabilized and remained at a near-constant depth. Any mathematical analysis of the results of pumping is complicated. After pumping begins, water that once would have entered the atmosphere will enter the well system. The amount of such water is small, but it helps to recover part of the drawdown caused by pumping. Therefore, before imposing a new stress on the existing system, it is important to study the present condition and the condition under which the existing waterlogging situation resulted. The study of steady-state conditions piror to canal irrigation and that of non-steady rise with time is prerequisite to evaluation of the hydrologic parameters of the flow system. Once the cause-and-effect relationship and the hydrologic factors involved are delineated, a new system may be superimposed on the existing conditions to identify the changes expected. In the following pages, the ground-water system in Chaj Doab is analyzed for the pre-irrigation period and for the period covering canal irrigation, up to 1960. The problem in the other adjacent Doab areas being nearly the same, the present study may also help in evaluating the problems involved in those areas. Boundary conditions in the area are not amenable to mathematical-model solution. Therefore, the electric-analog solution is attempted.

Available Data

Basically, the accuracy of the model study is determined by the amount of available information with respect to the complexity of the flow system. The accuracy of the analog model is tested by duplicating the known results of a known set of causes. The best cause-effect data available for this purpose are the water levels for a particular set of conditions. For this purpose, the required data was made available from the reports by the Water and Soils Investigation Division (WASID) of WAPDA (see bibliography). The following data has been used as a basic requirement to evaluate the electric-analog model.

1. Ground-water level contour map of Chaj Doab for the period prior to canal irrigation (figure 10).
2. Depth to water-table map for the pre-irrigation period (figure 11).
3. Location of main canals and their distributaries (figure 12).
4. Long-term hydrographs of few representative wells in Chaj Doab showing the rise in water levels with irrigation (figure 9).
5. Change map of ground water level rise for the period 1900 to 1960 (figure 13).
6. River-water levels at several points along the rivers Jhelum and Chenab (figure 12).
7. The average values for transmissibility and specific yield. The value for transmissibility has been taken as 400,000 gallons per day/foot and for specific yield as 0.25.

Analog Model Construction

An analog model for study of the laminar flow of water through porous media is developed by connecting generators that impose potential energy on networks which provide an energy-dissipative field. The assemblage of electronic components is commonly known as an analog computer. The network model simulates the geometry and internal state of the region and, thereby reproduces analogically the geology of the ground-water reservoir.

The basic electric-analog model for Chaj Doab was constructed by the United States Geological Survey's Analog Model Unit in Phoenix, Arizona. The model was constructed with a resistor spacing of one inch to simulate a field scale of one inch to one mile. It is a resistor-capacitor passive network and conforms to the methods of finite-difference approximation.

Scale Factors

The transformation of electrical data to its hydrologic equivalent or vice versa involves establishing certain scale factors as a prerequisite to the analog-model study. The choice of scale factors is governed by the size of the aquifer to be modeled, the time span under consideration, and the performance characteristics of the electronic equipment used. It was shown in chapter 3 that the equations

$$\nabla_x^2 h = \frac{Q_w}{q_w \Delta x^2} \cdot \frac{\partial h}{\partial t_w} \qquad (3.13)$$

and

$$\nabla_x^2 V = \frac{Q_E}{q_E \Delta x^2} \cdot \frac{\partial V}{\partial t_E} \tag{3.16}$$

for ground-water flow and electricity flow respectively are analogous. From these equations, the following scale factors (Bermes 1960) relating the two systems were obtained:

$$Q_w = K_1 Q_E \tag{4.1}$$

$$h = K_2 V \tag{4.2}$$

$$q_w = K_3 q_E \tag{4.3}$$

$$t_w = K_4 t_E \tag{4.4}$$

where

Q_w = Quantity of water in gallons

Q_E = Quantity of electricity in Coulombs

q_w = Rate of flow of water in gallons per day

q_E = Rate of flow of electricity in amperes

t_w = Time in days (actual)

t_E = Time in seconds (model)

Theoretically, the scale factors K_1 (gallons/Coulomb), K_2 (feet/volt), K_3 (gallons per day/ampere) and K_4 (days/second) may be chosen arbitrarily, because as long as $\frac{K_3 K_4}{K_1} = 1$, the two equations are equal and h (S, T, t) is known when V (C, R, t) is known. However, in the

solution of ground-water problems, where certain parameters range over many orders of magnitude, the choice of scale factors becomes limited. For the present study, the following scale factors were chosen to fit all the requirements:

$$K_1 = 10^{17} \text{ gallons/Coulomb} \tag{4.5}$$

$$K_2 = 10 \text{ feet/volt} \tag{4.6}$$

$$K_3 = 10^{11} \text{ gpd/ampere} \tag{4.7}$$

$$K_4 = 10^{6} \text{ days/second} \tag{4.8}$$

Analog Model Network Components

Equation 4.1; namely, $Q_w = K_1 Q_E$ expresses by definition, the quantitative equivalence of Coulomb's and Theis' equation. Substituting these relations into this equation results in a formula which may be used to determine the value of capacitor required to simulate storage. As expressed in chapter 2, the vertical permeability of the aquifer in Chaj Doab is very much smaller than the horizontal permeability and the ground-water flow is considered as two dimensional.

We have from equation 3.9,

$$S = \frac{Q_w}{\Delta h \, \Delta x \, \Delta y}$$

or

$$Q_w = S \, \Delta h \, \Delta x \, \Delta y \tag{4.10}$$

Substituting these two values of Q_w and Q_E in equation 4.1, it is found,

$$S \Delta x \Delta y \Delta h = K_1 C \Delta V$$

or

$$C = S \Delta x \Delta y \frac{\Delta h}{\Delta V} \frac{1}{K_1} \tag{4.11}$$

But from equation 4.2

$$\frac{\Delta h}{\Delta V} = K_2$$

equation 4.11 therefore becomes

$$C = S \Delta x \Delta y \frac{K_2}{K_1} \tag{4.12}$$

and for the units used, for an unconfined aquifer neglecting storage due to compression, equation 4.12 can be written as,

$$C \text{ (in farads)} = 7.48 \text{ (specific yield)} \Delta x \Delta y \frac{K_2}{K_1} \tag{4.13}$$

where Δx, Δy are the network spacings, measured parallel to the plane of flow, in feet.

For the present study, specific yield has been taken as 0.25, $\Delta x = \Delta y = 1$ mile $= 5280$ feet, and K_1, K_2 are defined by equations 4.5 and 4.6 respectively. Substituting these values in equation 4.13, the value for each capacitor is:

$$C = 7.48 \times 0.25 \times 5280 \times 5280 \times \frac{10}{10^{17}} = 0.005 \text{ micro farads.}$$

Similarly, the equation 4.3; i.e., $q_w = K_3 q_E$ expresses, by definition, the quantitative relation between Ohm's Law and Darcy's Law. Substitution

of these laws into the equation results in expressions that may be used to determine the values of a resistor required to simulate transmissibility. The following expressions are obtained:

$$R_x \text{ (Ohms)} = \frac{K_3}{K_2} \frac{\Delta x}{T \Delta y} \tag{4.14}$$

and

$$R_y \text{ (Ohms)} = \frac{K_3}{K_2} \frac{\Delta y}{T \Delta x} \tag{4.15}$$

For the finite difference network model of Chaj Doab $\Delta x = \Delta y = 1$ mile = 5280 feet, the resistors R_x and R_y shall be the same. The required magnitude of the network resistors, therefore, is

$$R \text{ (Ohms)} = \frac{K_3}{K_2} \frac{\Delta x}{T \Delta y} = \frac{K_3}{K_2} \frac{1}{T} \tag{4.16}$$

Substituting the values,

$$R = \frac{10^{11}}{K} \times \frac{1}{4 \times 10^5} = 22500 \text{ ohms}, \tag{4.17}$$

and for simplicity, resistors of value 22,000 ohms were used to construct the model.

Analysis for Steady-State Condition

The ground-water hydraulic system in the Chaj Doab was in a state of dynamic equilibrium under the natural environment that existed prior to the use of canal-irrigation systems. Considered over a reasonably long period of time, recharge to the ground-water reservoir balanced discharge and there was no evidence of long-term rise or decline of the

water table. The equilibrium conditions of the hydraulic system before irrigation are illustrated in figures 10 and 11. These figures show the altitude of water table above mean sea level, and the depth to the water table below land surface respectively. The equilibrium conditions of the ground-water regimen reflected the compound effects of many factors including geology, climate, topography and drainage on both the local and regional occurrence of ground water. The most interesting feature of the water-level contour map of figure 10 is the trough formed by the water table beneath Chaj Doab; and the marked flattening of the hydraulic gradient in the lower reaches, especially along the axis of the trough. The axis of the trough is in almost perfect alignment with the axis of the Doab. On the depth to water-table map (figure 11) the trough is reflected by the closed pattern of the contours which show increasing depth to the water table from the margins toward the center of the Doab. Thus, the general direction of ground-water movement was diagonally away from the rivers and downstream toward the axis of the Doab. The curving nature of ground-water level contours indicate that any underflow from upstream areas plus recharge from local precipitation did not quite balance underflow downstream and evapotranspiration and the equilibrium was maintained by the recharge from the rivers to the ground water.

Methodology and Results

Consideration of the above factors indicate that the rivers are the principal source of recharge and evapotranspiration discharge keep the system in dynamic equilibrium. In the analog-model analysis for steady-state conditions, the following assumptions were made:

1. The rivers are fully penetrating streams and are the recharge boundaries to the ground-water system.
2. Evapotranspiration is the principal discharge source to maintain equilibrium conditions. The term evapotranspiration as used here is in fact the actual evapotranspiration minus the areal recharge due to precipitation which is considered to be a very minor source of recharge.
3. Recharge by underflow from the upper reaches was considered negligible.

Accordingly, the rivers were simulated as constant potential boundaries with a gradient maintained according to the water levels in the rivers from upstream to downstream. Once this condition was established, the evapotranspiration on the whole network of the model could be controlled.

The apparatus used as an analog-model analyzer for the steady-state flow consisted of a group of variable power sources with potential divider arrangement, and a highly sensitive and accurate digital voltage meter with a reading scale for three decimal places. The digital voltmeter measured the potential drops in the network. A number of connecting leads served to finalize the circuit.

Fixed resistors of 470,000 ohms each were used vertically on the model net to simulate the evapotranspiration losses by imposing a negative voltage across these resistors and the model net. Each resistor representing the evapotranspiration effects occurring over a 16 square mile area was inserted at every fourth node point on the

model network. The value of 470,000 ohms was chosen by keeping in mind the working limitations of the available electrical equipment, the resistance values on the model network, and for maintaining low voltages on the net. Variable potentiometers were used to control the negative potentials on the evapotranspiration networks for finer adjustments. A block diagram of the assembly and the electric circuit of the analog computer is shown in figure 14 and in pictures, figures 15a, b. The capacitors on the model for this study were kept open circuit so as not to interfere with the steady-state condition.

After a few preliminary trials, the evapotranspiration network was broken into a more detailed pattern. This was done to control the negative voltages across the vertical evapotranspiration resistors more accurately. The final refined arrangement of evapotranspiration controls could simulate the field conditions on the model. The equipotential contours were drawn and were found to duplicate very closely the ground-water level contours of the pre-irrigation period (figure 16). On this map, the contours were shown after assigning to the electrical potential values the corresponding water-level values in accordance with the scale factors used. A comparison and similarity between figures 10 and 16 is evident.

The negative-voltage drop across each vertical resistor and the corresponding node point on the model network was then determined. The voltage drops and the relevant results calculated therefrom are given (Appendix A). This table shows the evapotranspiration rate in inches per year acting on each one foot square of ground-water surface. The

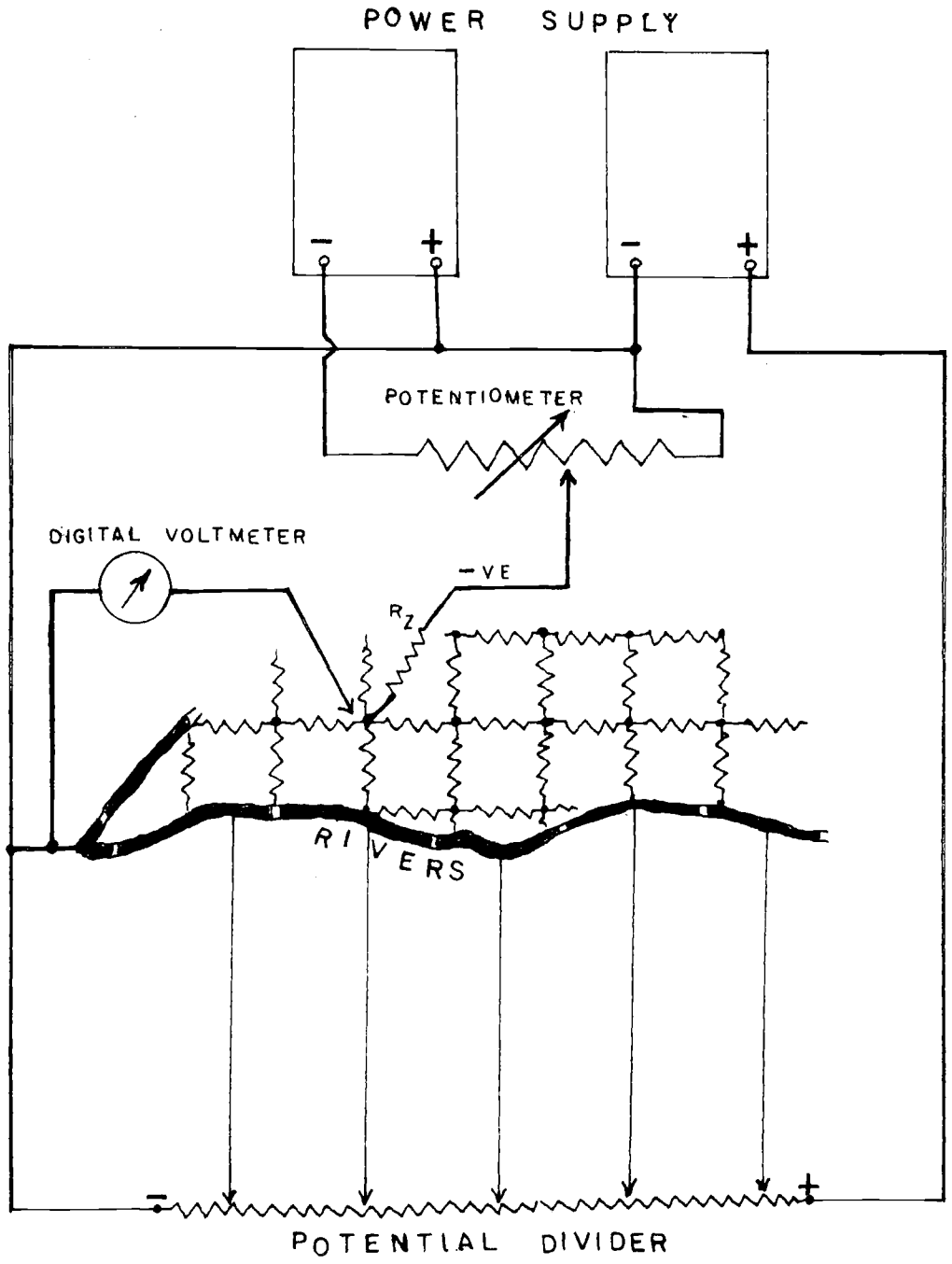

FIG·14 BLOCK DIAGRAM SHOWING COMPONENTS OF ANALOG COMPUTOR FOR STEADY STATE

Fig. 15a.--Showing Various Components of Analog Computer for Steady-State Conditions.

Fig. 15b.--Showing Net Resistors and Vertical Resistors for Evapotranspiration Effects

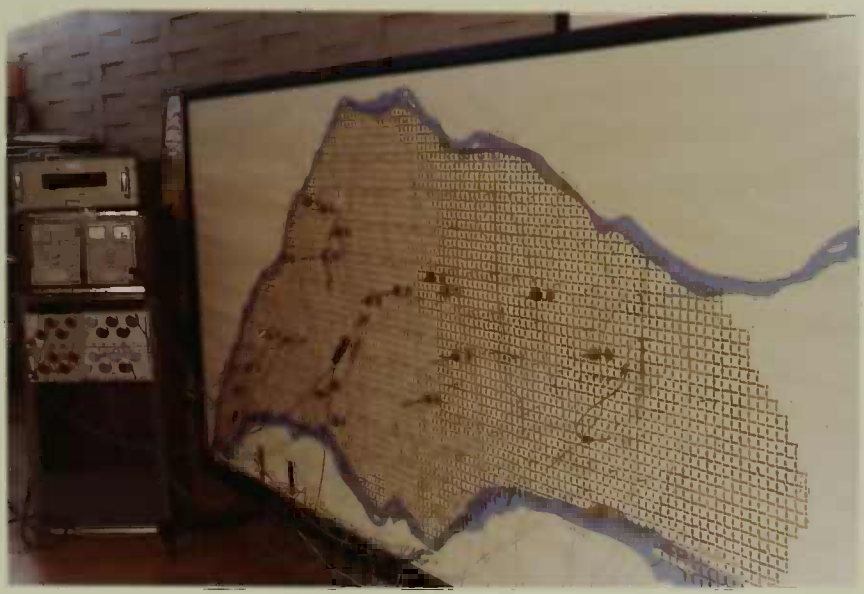

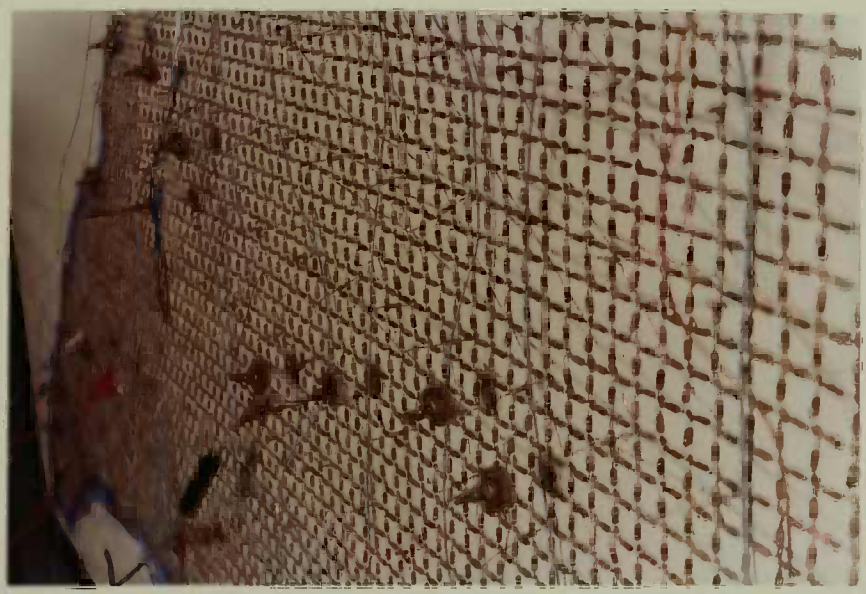

coordinates in the table refer to the node points on the grid where the vertical resistors were added. The reference to these is given in figure 17. The evapotranspiration rate values in terms of inches per year per square foot of ground-water surface have been plotted on map (figure 18) and are contoured. It is interesting to note that the evapotranspiration rates follow a reasonable pattern that correlates with depth of water table. Generally, the deeper the ground-water table from land surface, the smaller is the evapotranspiration rate.

From column 3 of Appendix A, the total evapotranspiration rate for the Chaj Doab area could be calculated. This value was 567.194×10^{-5} amperes or equivalent to 567.2 million gallons per day. Measuring the current flow from the ground-water network into the confluence point of the two rivers, a current of 0.012 milliamperes corresponding to 1.2×10^{6} gallons per day was found. This means that the rivers were recharging the ground water in the area at a rate of 568.4 million gallons per day, or 1.942 million gallons per day per mile length of the rivers. The analysis shows clearly the effect and influence of the rivers and that of evapotranspiration on the ground-water hydrologic system of Chaj Doab for the pre-irrigation period. Of a recharge rate of 568.4 million gallons per day from the rivers to the ground water, 567.2 million gallons per day were lost through evapotranspiration and 1.2 million gallons per day discharged again from the ground water to the rivers at the point of confluence.

Analysis For Non-Steady State Condition

The hydrologic conditions prevailing before the canal irrigation system as described in the previous section was changed then by the introduction of canal irrigation. The superposition of the canal system introduced additional factors of recharge that resulted in a rise of the water table in Chaj Doab. Since 1901 when the Lower Jhelum Canal system was opened, a general rise in water levels was observed. In 1915, the Upper Jhelum Canal system was also introduced, and this was superimposed on the respective areas of influence and resulted in rising trends of water levels. Figure 13 shows the fotal effect from both systems for the change in water levels from pre-irrigation to 1960. Typical hydrographs (figure 9) were presented in the earlier part of this chapter.

Methodology and Results

The rapid rise in the ground-water levels and then a gradual rate of decrease in rise effectively show the effect of evapotranspiration when water tables came quite close to the land surface. The study for this rise during the period over 60 years, first considering no evapotranspiration and then with the superposition of evapotranspiration on the ground-water hydrologic regimen, was the basis of this analysis. The analysis of the problem involves knowledge of the degree of hydraulic connection of the rivers, time sequence of canal construction, leakage from canals as a function of canal discharge, canal spacing density, and the effect of areal recharge owing to rainfall and underflow.

There is no data available for most of these items and the analysis, therefore, is based on certain assumptions for analog-model study. These assumptions are:

1. A complete hydraulic connection between the rivers and aquifer was assumed, and the level in the rivers was maintained at a constant head.
2. The transmissibility of the aquifer was considered to be uniform with an average value of 400,000 gallons per day per foot.
3. The specific yield was taken to be 0.25. This is somewhat higher than the average. This somewhat high figure was used on the assumption that the sediments above the water table were dry, or largely dry, prior to irrigation so that porosity is the actual model parameter.
4. Hydraulic connection between the canals and the aquifer was imperfect.
5. Initially, the leakage from canals was assumed according to the size of a particular canal and its discharge.
6. The areal recharge was neglected. In fact, the evapotranspiration rates used in the present analysis were based on the analysis made during the steady-state condition. These reflect the values of evapotranspiration rates minus the areal recharge.
7. Underflow from upper reaches of the Doab was considered to be negligible.

8. The sequence of the canal construction was followed. Map (figure 12) shows the location of canals. The canals were divided into segments and different recharges were imposed through various sections of the canals according to their sizes. Segments were marked on the map (figure 12).

The initial conditions for the non-steady state were considered as a potential of zero on the network at zero time.

The analog computer consisted of the passive resistance-capacitance network, the power supply, waveform generator, pulse generators, power amplifiers and oscilloscope. Two pulse generators were used; one for the Lower Jhelum Canal system with the duration corresponding to 60 years, and the other for the Upper Jhelum Canal system starting 15 years after with a total pulse length corresponding to a 45-year period. According to the power limitations of the analyzing equipment, with a maximum output of 100 volts, the resistors for the input of recharge through canals were calculated at the middle working voltage of 50 volts. This was done to have a reasonable range of control for input through the canals according to the requirements of the study. Resistors of different values to represent input recharge for different sections of the canals were used and were changed and adjusted as the situation demanded. The diagram showing the experimental set up is shown in figures 19, 19a, b, and 20a, b, c.

Analysis Without Evapotranspiration

The study for leakage from the canals over the period mentioned above was first made without any effect due to losses by evapotranspiration

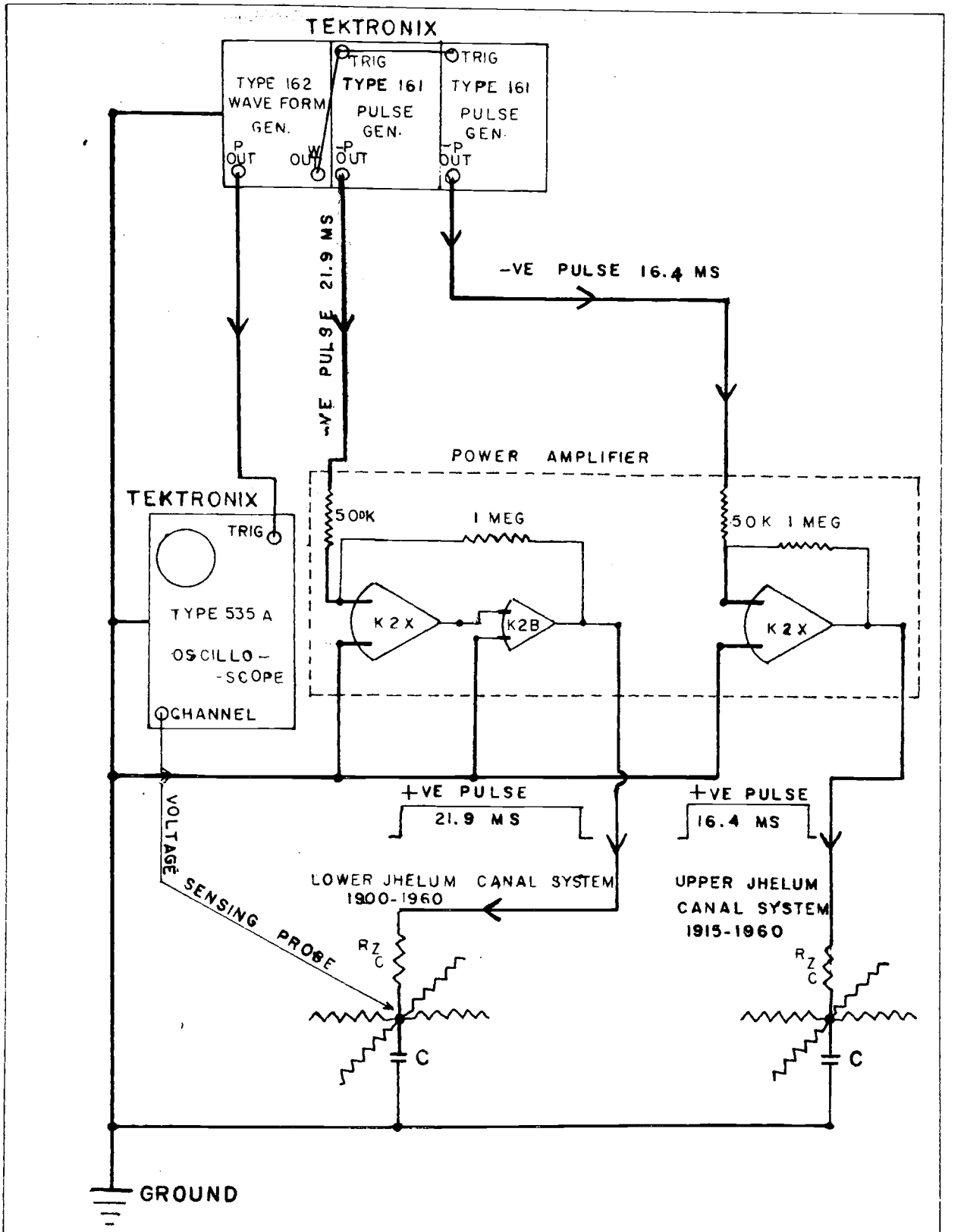

FIG·19 BLOCK DIAGRAM SHOWING COMPONENTS OF ANALOG COMPUTOR FOR NON-STEADY STATE

Fig. 19a.--Circuit Diagram for Study of Non-Steady State Without The Effect of Evapotranspiration.

Fig. 19b.--Circuit Diagram for the Study of Non-Steady State With the Effect of Evapotranspiration.

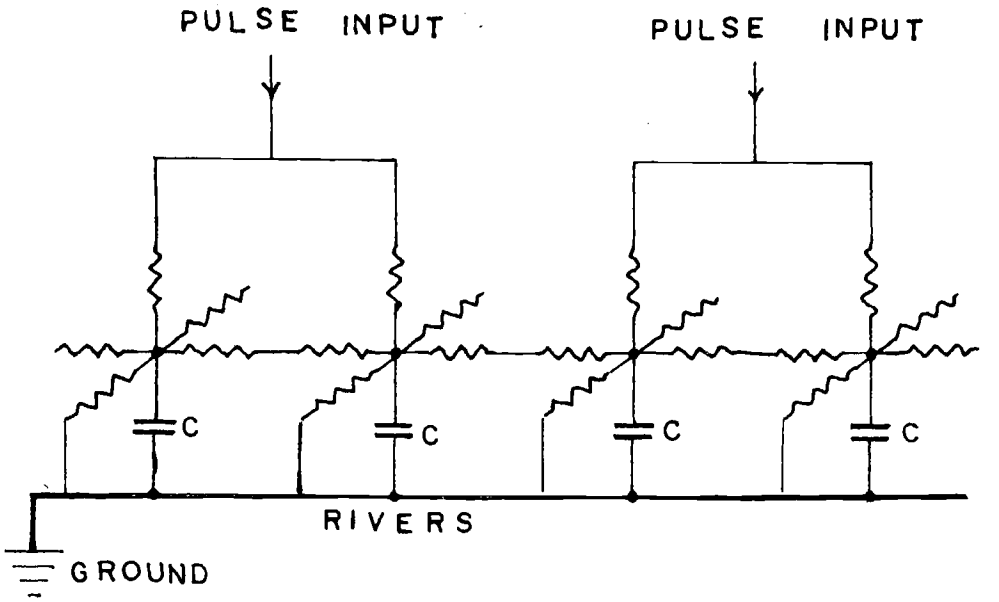

FIG. 19-a.

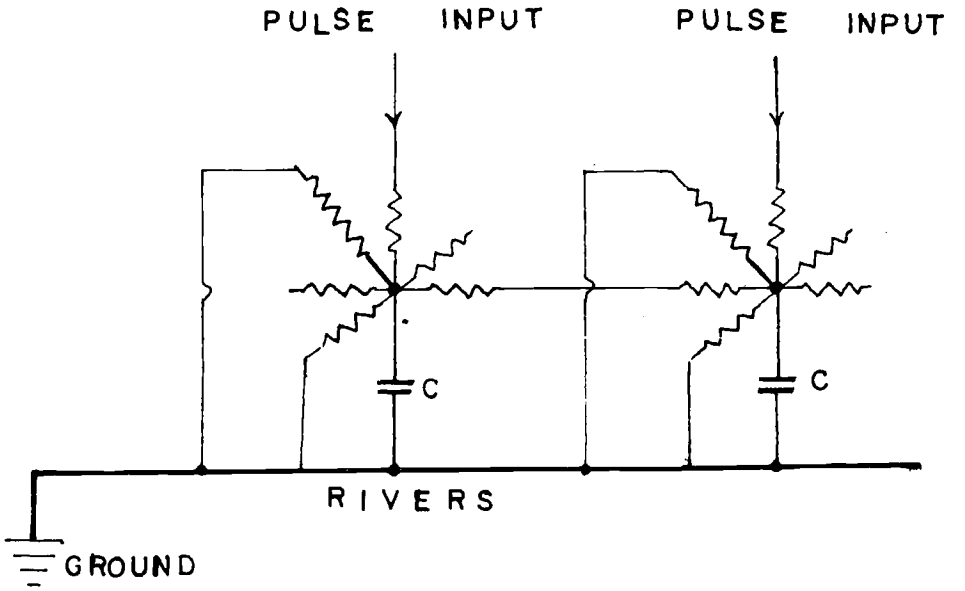

FIG. 19-b.

Fig. 20a & 20b.--Showing Experimental Set-up of Various Components of Analog Computer for Non-Steady State Conditions.

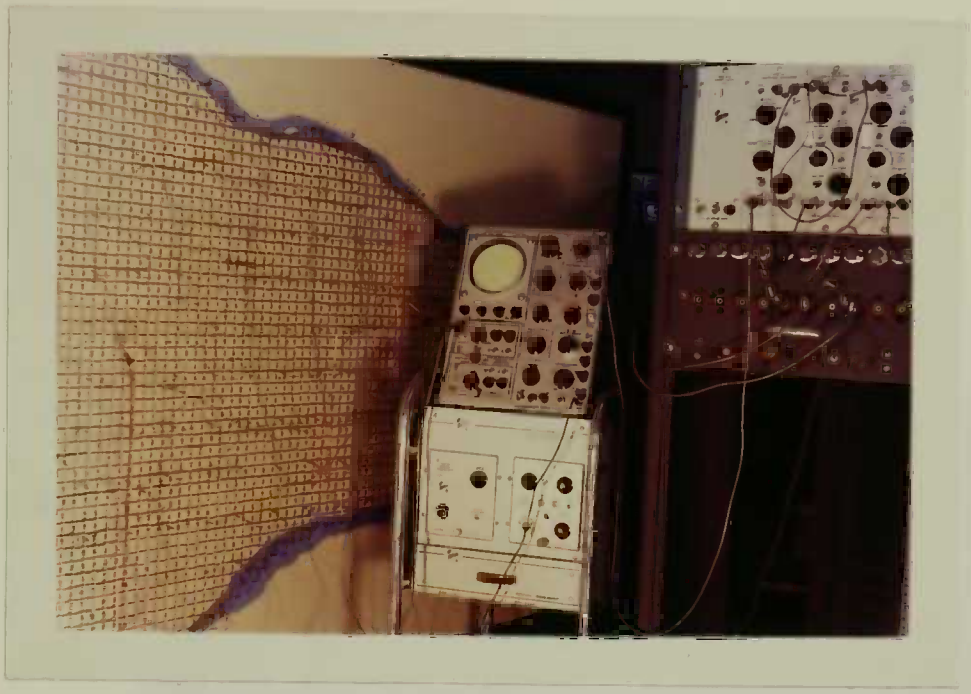

Fig. 20c.--Showing the Arrangement of the Capacitors of Electric-Analog Model for Non-Steady State Condition.

from the ground-water reservoir. This was done in order to evaluate the net rate of addition of water to the ground-water reservoir during the complete period, considering leakage from the canals as the source. Adjusting the recharge rate from various sections of the canals, according to their sizes, a change map for the rise in ground-water levels corresponding to period from 1900 to 1960 was prepared (figure 21). The observed values from the analog model agree very closely with the field data (figure 13). The accretion rates from various canal segments to the ground water and those given per mile length of canal were calculated are tabulated in Appendix B. The final column in Appendix B gives the values of rate of accretion through the various segments in terms of cubic feet per second per mile length of the particular canal.

From this study, it was found that the net rate of accretion to the ground-water reservoir occurring only as a result of canal seepage is 900.3 million gallons per day.

Analysis with Evapotranspiration Effects

The well hydrographs (figure 9) show that the rise in ground-water levels was quite uniform for the first 20 to 30 years, after which the rise became non-linear. The linear portion exhibits the period when the effect of evapotranspiration was comparatively small on the whole. After this period of linear rise in water table, the effect of evapotranspiration on the water table became quite prominent. Determination of the rate of evaporation applicable all over the Chaj Doab presented some difficulty. However, from the studies made on analog

models for the evapotranspiration during the steady-state analysis of the problem, it was found that the rate of evaporation was a function of depth to water. A correlation of the evapotranspiration-contour map (figure 18) and the depth to water map prior to irrigation (figure 11) yielded various curves applicable in different parts of the Chaj Doab. These curves plotted for depth versus rate of evaporation (figure 22) show distinct relation between evaporation and depth to water table. The slope of the steep portion on these curves, which defines the maximum rate of evaporation that occurred when the water table was close to the land surface, was used as the rate of evaporation occurring in the respective areas. The slope of the curve gives the evapotranspiration rate in inches per year per foot of depth. Using the scale and conversion factors, these rates for different portions of Chaj Doab were converted into electrical equivalents in amperes per volt. The various areas with different rates of evaporation are shown in figure 23. The required resistors thus were calculated for each different portion of Chaj Doab for appropriate application of discharge through evaporation. The resistors were inserted vertically on the analog-model network at every fourth node point to represent an area of 16 square miles being affected by each resistor.

The imposition of evapotranspiration conditions automatically required more voltage input for canal recharge effect. Inacreasing the voltage by the required amount and simulating recharge input through the canals, the changes in water levels in the Doab were observed on oscilloscope screens. The observations agreed very closely with those

Fig. 22.--Curves Showing Evapotranspiration Rates Versus Depth to Water Table for Chaj Doab - Analog Model.

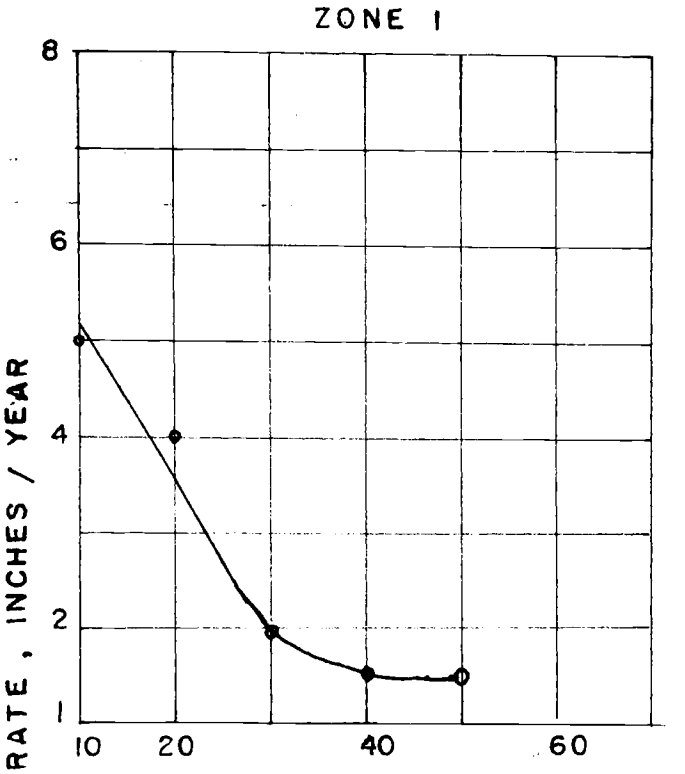

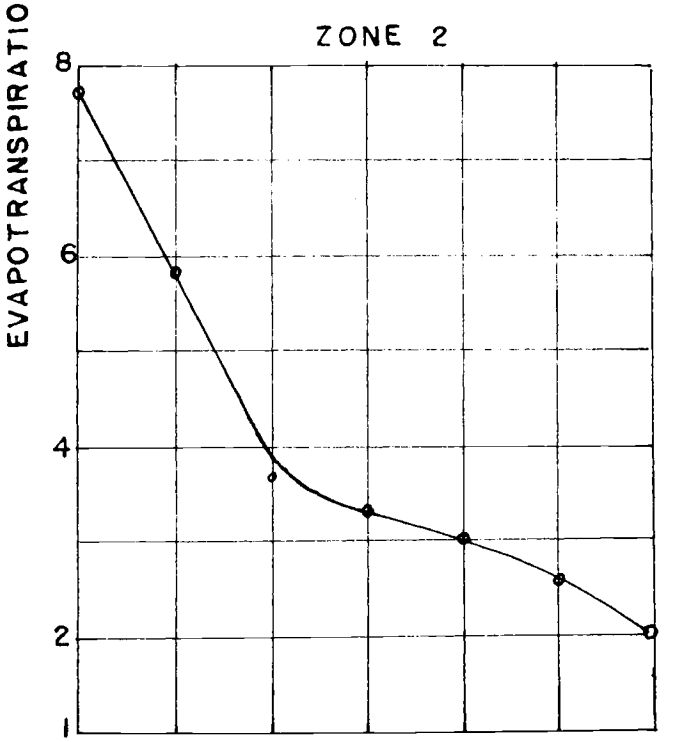

FIG. 22 ANALOG MODEL

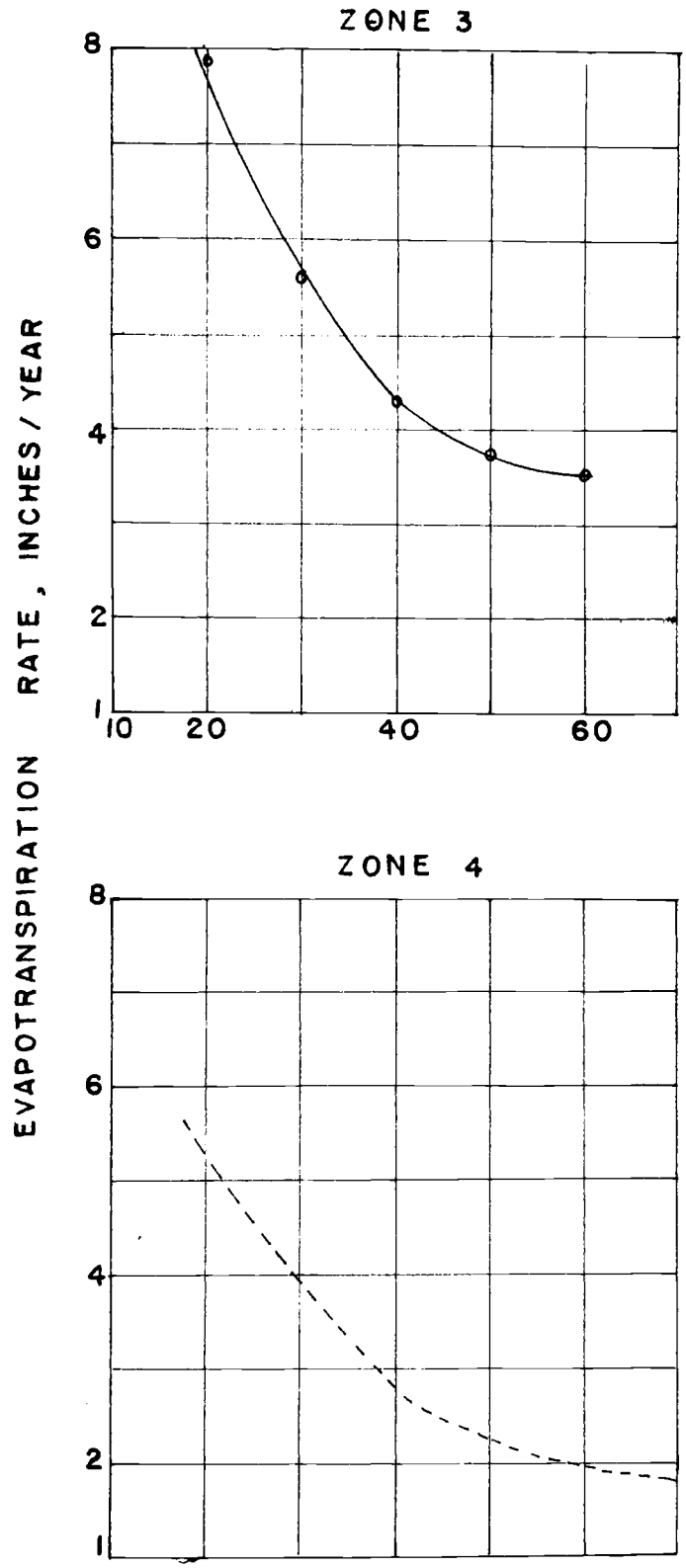

FIG·22 ANALOG MODEL

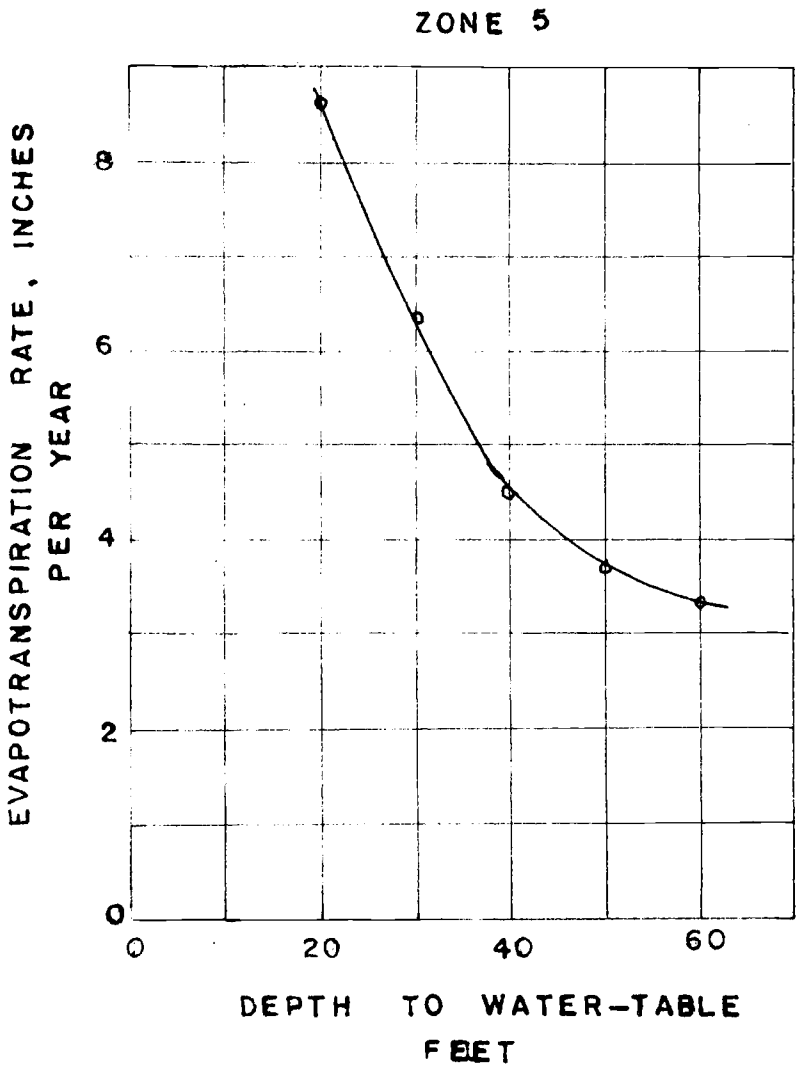

FIG.22

ANALOG MODEL

from field observations. Figure 24 shows the change map obtained from the analog studies and this is comparable with that of figure 13. Some of the hydrographs, as converted from their electrical equivalents to the hydrologic components, observed on the oscilloscope screen are shown in figure 25a to e. These hydrographs clearly show various effects. Figure 25a, b shows the effect of Upper Jhelum Canal system and its superposition on the already existing Lower Jhelum Canal system. Figure 25c shows very little rise near the rivers. Figures 25d, e show the general type hydrographs in other areas of the Doab. A general resemblance of these observed hydrographs with those of field data is noted.

The results for the rate of recharge to the ground-water system from canal leakage as calculated are tabulated in Appendix C. This appendix gives the total rate of leakage per unit length of various segments of the canals. The seepage values per mile of canal are incorporated in figure 12.

The total rate of leakage from all canals as a whole as calculated from Appendix C is 1767.6 million gallons per day. The total current flowing out through the evapotranspiration resistors was measured and found to be 8.675 milliamperes which corresponds to a discharge rate of 867.5 million gallons per day.

Using these two figures of 1767.6×10^6 gallons per day as leakage from the canals and 867.5×10^6 gallons per day as loss due to evapotranspiration, the net recharge to the ground-water system would be 900.1 million gallons per day.

Fig. 25a & b.--Hydrographs Showing Effect of Upper Jhelum Canal System and Its Superposition on the Already Existing Lower Jhelum Canal System - Analog Model.

Coordinates of Node Point for Fig. 25

a. 27, I

b. 30, E

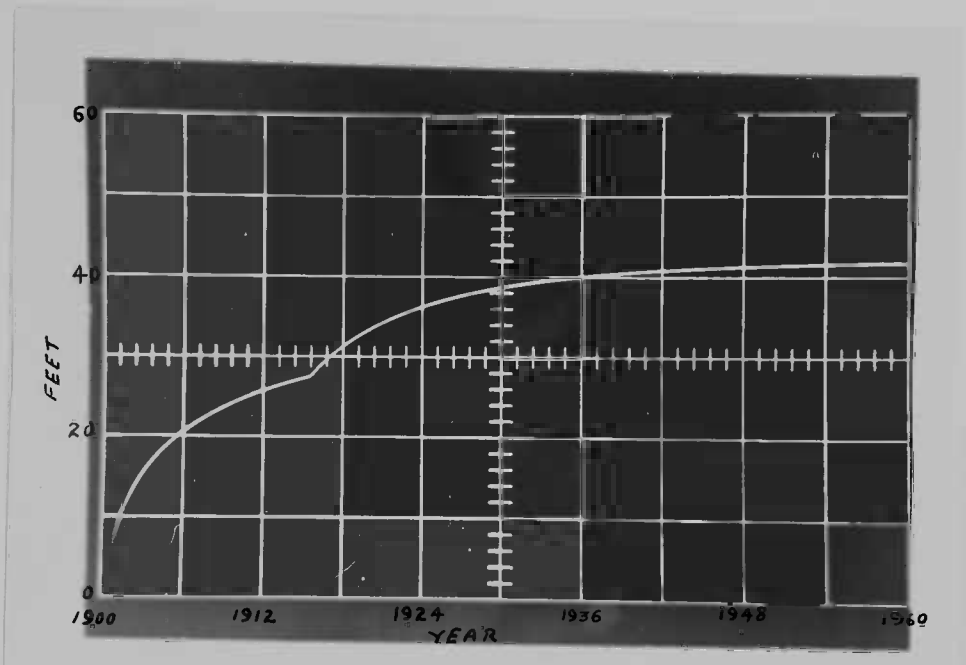
60
40
20
0
FEET
1900
1912
1924
1936
1948
1960
YEAR

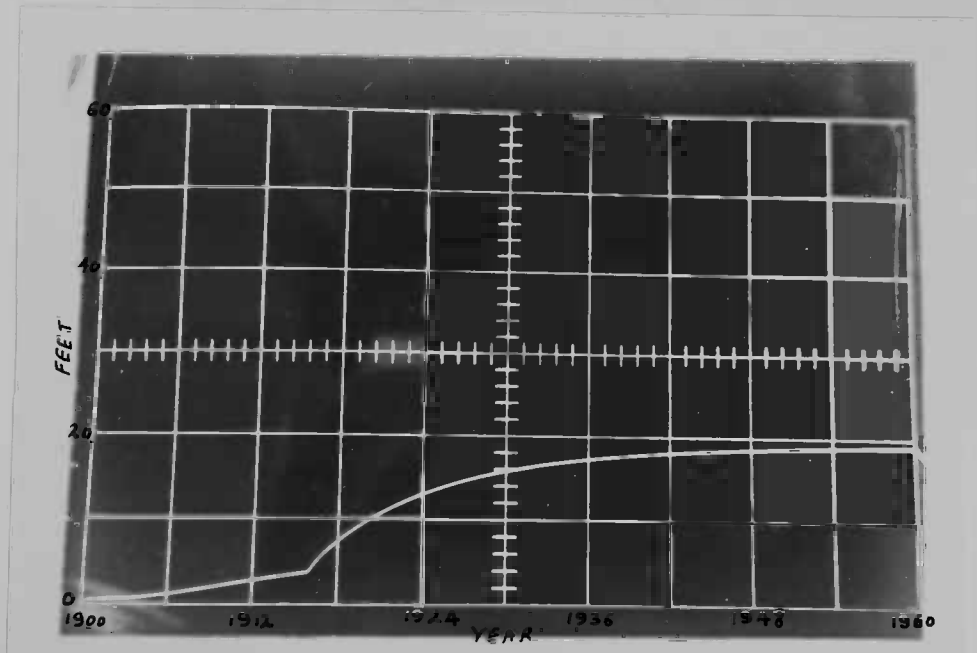
60
40
20
0
FEET
1900
1912
1924
1936
1948
1960
YEAR

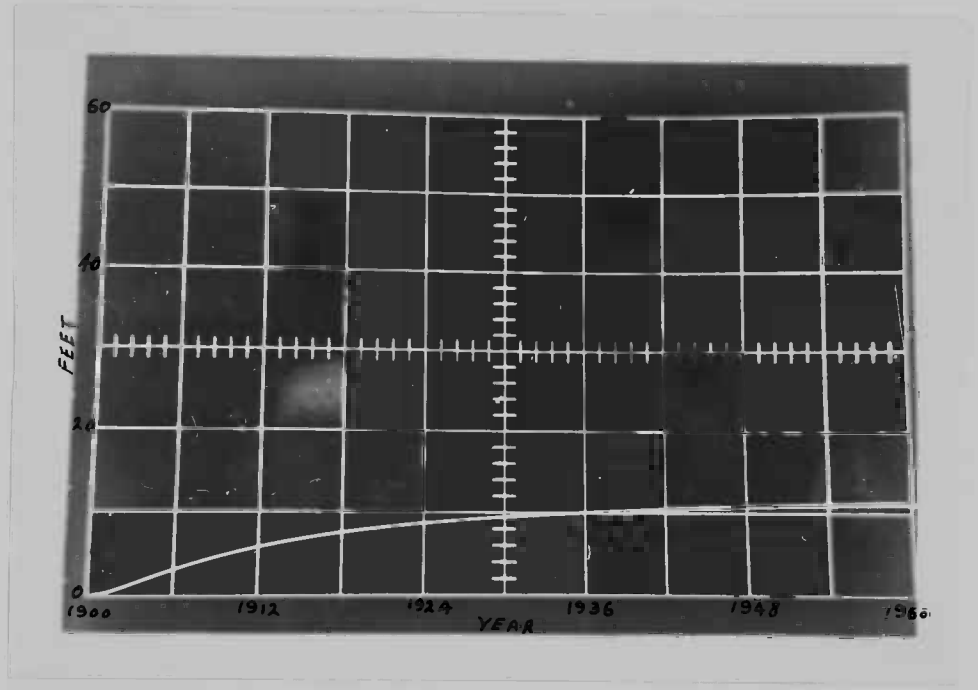

Fig. 25c.--Hydrograph Showing Very Little Rise In Ground-Water Level Due to Location Near the River - Analog Model.

Coordinates of Node Point 6, F.

Fig. 25d & e.--Showing the General Type of Hydrographs In Central Portions of Chaj Doab - Analog Model

Coordinates of Node Point for Fig. 25

d. 18, I

e. 21, G

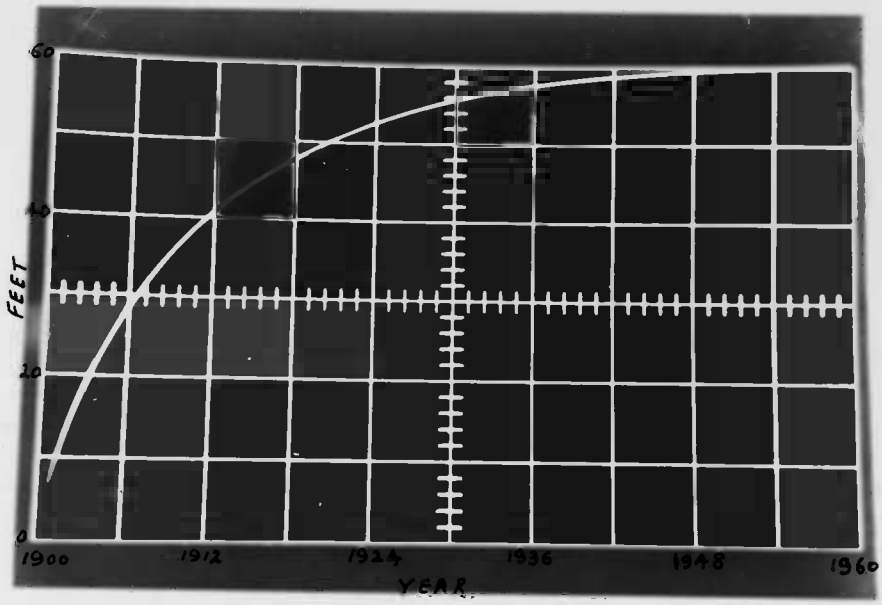
60
40
20
0
FEET
1900
1912
1924
1936
1948
1960
YEAR

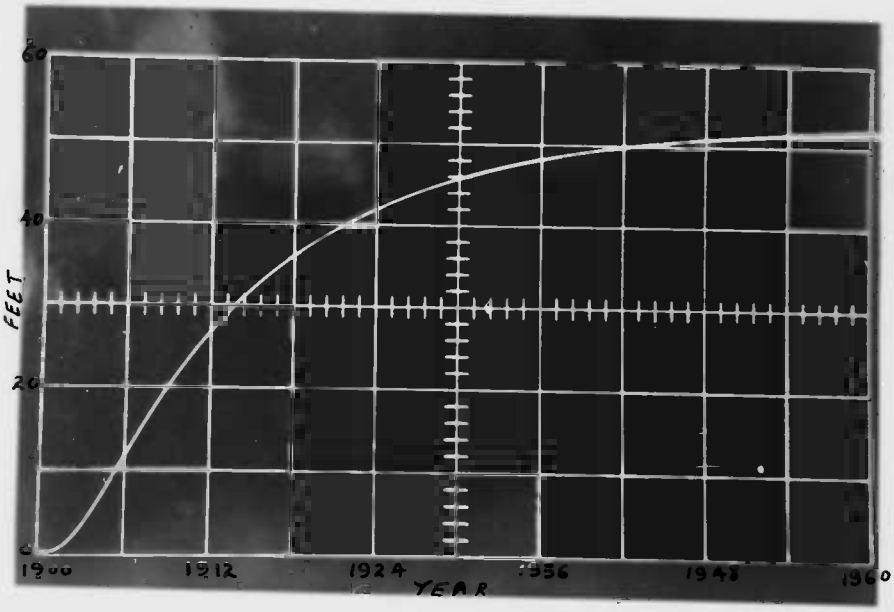
60
40
20
0
FEET
1900
1912
1924
1936
1948
1960
YEAR

In the earlier analysis leakage from the canals was 900.27×10^6 gallons per day and evaporation was not considered and the net recharge to the ground-water system was 900.27×10^6 gallons per day or essentially the same net recharge as the second analysis. This indicates the fairness of the accuracy of model and results, showing the close simulation of field conditions and the feasibility of the assumptions made for the analog analysis.

CONCLUSIONS

On the basis of the electric-analog analysis of the ground-water system in Chaj Doab, the following points are concluded:

1. During the pre-irrigation period, rivers were the major source of recharge to the ground water, recharging at a rate of the order of 2 millions gallons per day per mile of the river length. The total recharge rate from Jhelum and Chenab Rivers was 568 million gallons per day.
2. The major discharge of ground water from Chaj Doab to keep the hydraulic dynamic equilibrium during the pre-irrigation period was evapotranspiration. The areal recharge from precipitation was less than the evapotranspiration. The total discharge from ground water of the area through evapotranspiration was of the order of 567 million gallons per day. The rest of the ground water; namely, 1.2 million gallons per day was being discharged from the ground water to the rivers at the point of confluence.
3. The results show that evaporation losses were heaviest adjacent to the rivers, where the water table was closest to the land surface.
4. The evaporation rates were directly proportional to the depth to water table below land surface and were of the order of

less than 2 inches per year in the center of the Doab where the depth to water table was beyond 60 feet.

5. The configuration of the water table in Chaj Doab was controlled by the pattern of evapotranspiration losses and by the geometry of the Doab.
6. The recharge by underflow from upper reaches of the Doab was negligible as compared to the recharge from the rivers.
7. The main source of rise of ground-water levels in Chaj Doab is the seepage from the canal-irrigation system and is the principal cause of subsurface-drainage problems in the area. Also this is a major component of ground-water recharge. The net rate of accretion to the ground-water reservoir is of the order of 900 million gallons per day.
8. The net rate of leakage from the canals is of the order of 1767 million gallons per day. Of this 867 million gallons per day is the loss due to evapotranspiration.
9. The leakage from the canals is a function of the size and discharge in the canal.
10. Movement of the water from the canal to the water table is also controlled by the permeability of the canal boundary and the hydraulic gradient from canal to aquifer. This inference is made on the behavior of main Lower Jhelum Canal in its first few miles, where besides its size and discharge, the seepage from it in that portion is relatively small. In this area the ground-water level is high and the hydraulic gradient from the

river Jhelum is limited. In addition, formation in this area is less permeable.

11. The canal irrigation has changed and modified the flow regimen of rivers, as the rivers are no longer the principal recharge boundaries to the ground-water reservoir.

The conclusions of the present study are based on certain basic assumptions as described in chapter 4. However, similar results would be achieved using other possible factors and conditions. The assumptions made by the author looked more appropriate to him. Nevertheless, the analyses and the assumptions made during the present study give a reasonable picture of what situation might have persisted over the long period of irrigation history. The present study, therefore, provides an opportunity and a point of thought for the engineer looking for the effects of the environmental controls involved in the problem of water-logging and identifies possible solutions. The analyses made and the conclusions gained establish guidelines for any further work. It is the sincere desire of the author that the conclusions arrived in the present work are not to be considered as completely definitive, but rather as establishing magnitudes and guidelines for future study.

APPENDIX A

Evapotranspiration Rates For Pre-Irrigation Period

1	2	3	4	1	2	3	4
2,A	16.237	3.459	4.560	I	8.959	1.906	2.310
B	16.402	3.495	4.610	J	20.763	4.415	2.516
3,B	16.654	3.542	4.680	12,E	7.915	1.674	5.830
C	16.803	3.575	4.695	F	4.534	0.963	2.210
4,B	17.608	3.753	4.950	G	7.139	1.518	1.270
C	17.107	3.642	4.180	H	7.899	1.680	2.020
D	17.383	3.693	4.870	I	8.796	1.870	2.220
5,C	19.514	4.153	5.490	J	20.449	4.360	2.466
D	16.683	3.542	4.680	13,C	21.199	4.510	5.950
E	17.915	3.812	5.030	D	9.352	1.911	2.522
6,C	18.366	3.900	5.150	E	6.645	1.411	1.865
D	16.895	3.590	4.745	F	4.589	0.975	1.288
E	17.000	3.613	4.760	G	7.387	1.570	2.073
F	18.504	3.933	5.190	H	8.062	1.718	2.265
7,C	18.080	3.842	5.080	I	8.512	1.811	2.393
E	14.208	3.026	4.000	J	9.685	2.060	2.720
F	17.589	3.740	4.940	K	11.539	2.452	3.237
G	19.292	4.106	5.410	14,C	21.174	4.500	5.946
8,E	14.511	3.302	4.360	D	8.401	1.790	2.360
F	7.044	1.497	1,975	E	5.901	1.260	1.660
G	18.507	3.938	5.190	F	4.934	1.050	1.386
9,D	18.065	3.840	5.060	G	4.825	1.025	1.350
E	7.104	1.512	1.998	H	7.822	1.667	2.200
F	7.000	1.490	1,967	I	8.670	1.845	2.435
G	7.797	1.658	2.186	J	9.322	1.985	2.620
H	19.690	4.185	5.510	K	10.295	2.188	2.890
10,D	18.542	3.946	5.206	L	12.586	2.675	3.530
E	7.466	1.590	2.100	M	26.754	5.260	6.950
F	7.063	1.503	1.986	15,B	22.591	4.800	6.340
G	7.723	1.643	2.170	C	9.578	2.040	2.683
H	8.326	1.780	2.350	D	7.925	1.605	2.222
I	19.922	4.245	5.600	E	5.909	1.260	1.660
11,D	19.761	4.200	5.250	F	5.313	1.130	1.487
E	7.462	1.590	5.550	G	5.041	1.073	1.416
F	6.829	1.451	2.100	H	5.573	1.185	1.565
G	7.454	1.587	1.918	I	8.302	1.765	2.330
H	8.219	1.750	2.093	J	9.549	2.030	2.680

15,K	10.367	2.201	2.904
L	11.551	2.456	3.240
M	25.121	5.340	7.090
16,B	23.331	4.962	6.550
C	10.140	2.150	2.840
D	7.176	1.526	2.014
E	6.375	1.357	1.790
F	5.755	1.228	1.620
G	5.482	1.168	1.540
H	5.723	1.217	1.605
I	6.283	1.338	1.765
J	9.195	1.955	2.580
K	10.716	2.280	3.010
L	11.932	2.538	3.350
M	25.509	5.425	7.150
17,B	24.389	5.170	6.825
C	10.785	2.287	3.020
D	7.733	1.643	2.170
E	6.896	1.456	1.920
F	6.260	1.332	1.760
G	5.972	1.270	1.677
H	6.051	1.290	1.701
I	6.470	1.377	1.816
J	9.685	2.060	2.720
K	11.223	2.486	3.282
L	12.525	2.662	3.520
M	26.253	5.580	7.360
18,B	24.735	5.252	6.930
C	10.553	2.290	3.024
D	8.362	1.780	2.350
E	7.506	1.598	2.105
F	6.819	1.450	1.912
G	6.534	1.388	1.830
H	6.620	1.410	1.860
I	7.052	1.501	1.980
J	10.287	2.286	3.020
K	11.899	2.530	3.340
L	13.236	2.820	2.720
M	26.982	5.730	7.555
19,B	25.281	5,375	7.100
C	12.135	2.582	3.410
D	9.109	1.950	2.578
E	8.174	1.738	2.293
F	7.314	1.556	2.054
G	7.335	1.560	2.060
H	7.416	1.580	2.083
I	8.012	1.705	2.250
J	11.013	2.342	3.096
19,K	12.789	2.716	3.580
L	15.362	3.266	4.310
M	27.319	5.820	7.690
20,B	26.691	5.670	7.490
C	13.259	2.820	3.720
D	11.273	2.498	3.298
E	8.981	1.910	2.520
F	8.053	1.714	2.262
I	8.736	1.857	2.650
J	11.829	2.520	3.325
K	13.819	2.941	3.880
L	16.911	3.600	4.750
21,C	26.747	5.680	7.500
D	12.419	2.642	3.490
E	9.899	2.102	2.780
F	8.813	1.876	2.476
G	8.691	1.850	2.542
H	9.079	1.930	2.543
I	9.469	2.012	2.655
J	13.359	2.840	3.750
K	14.870	3.160	3.170
L	29.062	6.180	8.150
22,D	14.437	3.072	4.050
E	10.826	3.402	3.040
F	10.064	2.140	2.823
G	9.740	2.067	2.730
H	9.796	2.085	2.758
I	10.223	2.178	2.875
J	14.141	3.010	3.970
K	15.640	3.325	4.390
L	29.054	6.180	8.150
23,D	15.539	3.306	4.360
E	12.011	2.555	3.338
F	10.929	2.321	3.070
G	10.544	2.240	2.960
H	10.592	2.250	2.970
I	11.049	2.350	3.100
J	15.016	3.197	4.210
K	16.429	3.497	4.610
L	29.492	6.280	8.300
24,D	28.579	6.070	8.020
E	14.240	3.030	4.000
F	12.079	2.566	3.390
G	11.442	2.435	3.213
H	11.505	2.446	3.230
I	11.969	2.540	3.355
J	15.992	3.390	4.480
K	18.723	3.980	5.250

25,D	29.672	6.310	8.345	27,G	13.889	2.950	3.895
E	16.119	3.430	4.530	H	14.129	3.010	3.970
F	12.204	2.601	3.440	I	14.829	3.158	4.160
G	12.436	2.646	3.497	J	32.259	6.875	9.080
H	12.530	2.670	3.522	28,E	19.126	4.065	5.365
I	15.408	3.280	4.330	F	14.876	3.160	4.170
J	17.212	3.665	4.845	G	14.905	3.170	4.190
K	20.225	4.300	5.670	I	31.804	6.770	8.950
26,D	31.134	6.620	8.740	J	33.459	7.120	9.400
E	17.175	3.657	4.825	29,E	19.971	4.245	5.600
F	15.314	3.263	4.308	F	16.153	3.439	4.540
I	13.590	2.885	3.808	G	15.956	3.390	4.480
J	30.439	6.490	8.560	H	16.371	3.480	4.596
27,E	18.186	3.870	5.104	I	33.141	7.040	9.300
F	16.266	3.460	4.560				

NOTE: Column 1 - Co-ordinates of the node point.
Column 2 - Negative voltage across the vertical (E.T) resistor and the corresponding node on the model network.
Column 3 - Current flowing Through vertical resistor ($x10^{-5}$ amperes).
Column 4 - Evapotranspiration rate in inches per year per square foot.

APPENDIX B

Leakage From Canals Without Evapotranspiration Effects

1	2	3	4	1	2	3	4
1	47,000	0.850	4.85	18	122,000	0.336	3.20
2	78,000	0.512	8.00	19	77,000	0.520	8.06
3	57,000	0.701	3.63	20	192,000	0.208	4.03
4	86,000	0.465	3.22	21	90,000	0.444	4.31
5	736,000	0.054	0.35	22	154,000	0.260	4.02
6	192,000	0.208	3.22	23	96,500	0.415	2.38
7	230,000	0.174	1.61	24	139,000	0.388	1.93
8	437,000	0.092	0.81	25	54,000	0.741	4.00
9	748,000	0.054	0.80	26	134,000	0.298	1.61
10	192,000	0.208	1.61	27	440,000	0.078	2.02
11	372,700	0.107	1.59	28	348,000	0.099	0.68
12	876,000	0.046	0.40	29	218,000	0.158	1.02
13	485,000	0.082	0.40	30	218,000	0.158	1.02
14	65,000	0.614	3.98	31	372,000	0.093	0.69
15	190,000	0.210	2.41	32	162,000	0.213	2.06
16	440,000	0.091	0.80	33	162,000	0.213	1.37
17	736,000	0.054	0.71				

NOTE: Column 1 - Designation of the canal segiments.
Column 2 - Resistance in ohms along the respective segment.
Column 3 - Current flowing through the resistor ($x10^{-3}$ amperes).
Column 4 - Leekage from the canal segments in cubic feet per second per mile length of the respective segment.

Voltage for segments 1 to 26 = 40 volts
Voltage for segments 27 to 33 = 34.5 volts

APPENDIX C

Leakage From Canals With Evapotranspiration Effects

1	2	3	4	1	2	3	4
1	47,000	1.660	9.46	18	122,000	0.640	6.20
2	78,000	1.000	15.50	19	77,000	1.012	15.70
3	57,000	1.370	7.08	20	192,000	0.406	7.87
4	86,000	0.908	6.30	21	90,000	0.860	8.30
5	736,000	0.106	.69	22	154,000	0.506	7.85
6	192,000	0.406	6.30	23	96,500	0.807	4.62
7	230,000	0.390	3.60	24	139,000	0.560	3.78
8	437,000	0.178	1.57	25	54,000	1.441	7.76
9	748,000	0.104	1.56	26	134,000	0.582	3.14
10	192,000	0.406	3.15	27	440,000	0.159	4.10
11	372,700	0.210	3.13	28	348,000	0.201	1.40
12	876,000	0.089	0.78	29	218,000	0.322	2.08
13	485,000	0.160	0.78	30	218,000	0.322	2.08
14	65,000	1.200	7.75	31	372,000	0.188	1.40
15	190,000	0.410	4.68	32	162,000	0.437	4.22
16	440,000	0.177	1.55	33	162,000	0.637	4.82
17	736,000	0.106	1.37				

NOTE: Column 1 - Designation of the canal segments.
Column 2 - Resistance in ohms along the respective segment.
Column 3 - Current flowing through the resistor ($x10^{-3}$ amperes).
Column 4 - Leakage from the canal segments in cubic feet per second per mile length of segment.

Voltage for segments 1 to 26 = 78 volts.
Voltage for segments 27 to 33 = 70 volts.

SELECTED BIBLIOGRAPHY

Bennett, G. D., Rehman, A. R., Sheik, I. A., and Ali, S., 1964, Analysis of aquifer tests in the Punjab region of West Pakistan: West Pakistan Water and Power Development Authority, Water and Soils Investigation Division.

Bermes, B. J., 1960, An electric analog method for use in quantitative hydrologic studies: U. S. Geol. Survey, Ground Water Branch, Phoenix, Ariz.

Carlston, C. W., 1953, History and causes of rising ground-water levels in the Rechna Doab: United Nations, FAO Report no. 90.

Gilani, M. A. S., and Hamid, A., 1960, Quality of ground water, Chaj Doab: West Pakistan Water and Power Development Authority, Water and Soils Investigation Division, Basic Data Release no. 2.

Greenman, D. W., Swarzenski, W. V., and Bennett, G. D., 1963, The ground-water hydrology of the Punjab West Pakistan: West Pakistan Water and Power Development Authority, Water and Soils Investigation Division, Bull. no. 6.

Jacob, C. E., 1950, Flow of ground water, in Rouse, Hunter, Engineering hydraulics: John Wiley and Sons, Inc., New York.

Karplus, W. J., 1958, Analog simulation. New York: McGraw Hill Book Company.

Kidwai, Zamir-un-Din, 1962, The geology of Rechna and Chaj Doabs, West Pakistan: West Pakistan Water and Power Development Authority, Water and Soils Investigation Division, Bull. no. 5.

Midha, D. C., Luthra, H. R., and Vaidhianethan, V. I., 1937, A new method of determining seepage from canals in areas of high water table: Punjab Irrigation Research Institute, Research Pub., v. V, no. 7.

Sheikh, I. A., and Hussain, A., 1960, Analysis of precipitation data from Rechna, Chaj, and Thal Doabs: West Pakistan Water and Power Development Authority, Water and Soils Investigation Division, Tech. Paper no. 1.

Shakur, M.A., Hussain, A., and Rehman, A.R., 1960, Records of ground-water levels, Chaj Doab: West Pakistan Water and Power Development Authority, Water and Soils Investigation Division, Basic Data Release no. 5.

Skibitzke, H. E., 1960, Electronic computers as an aid to the analysis of hydrologic problems: Pub. no. 52 of the I.A.S.H. Comm. of Subterranean Water, p. 347-358.

Skibitzke, H. E., 1963, The use of analog computers for studies in ground-water hydrology: The Geol. Soc. of London, The Inst. of Water Engineers, v. 17, no. 3.

Theis, C. V., 1935, The relation between the lowering of Piezometric surface and the rate and duration of discharge of a well using ground-water storage: Am. Geophys. Union Trans. pt. 2, p. 519-524 (August).

Theis, C. V., 1938, The significance and nature of the cone of depression in ground-water bodies: Econ. Geology, v. 33, no. 8, p. 889-902 (December).

Wilsdon, B. H., and Bose, N. K., 1934, A gravity survey of the sub-alluvium of the Jhelum - Chenab - Ravi Doabs and its application to problems of water-logging: Memoirs, Punjab Irrig. Research Inst., v. VI, no. 1.

In Pocket:

Fig. 6
7
10
11
12
13
16
17
18
21
23
24

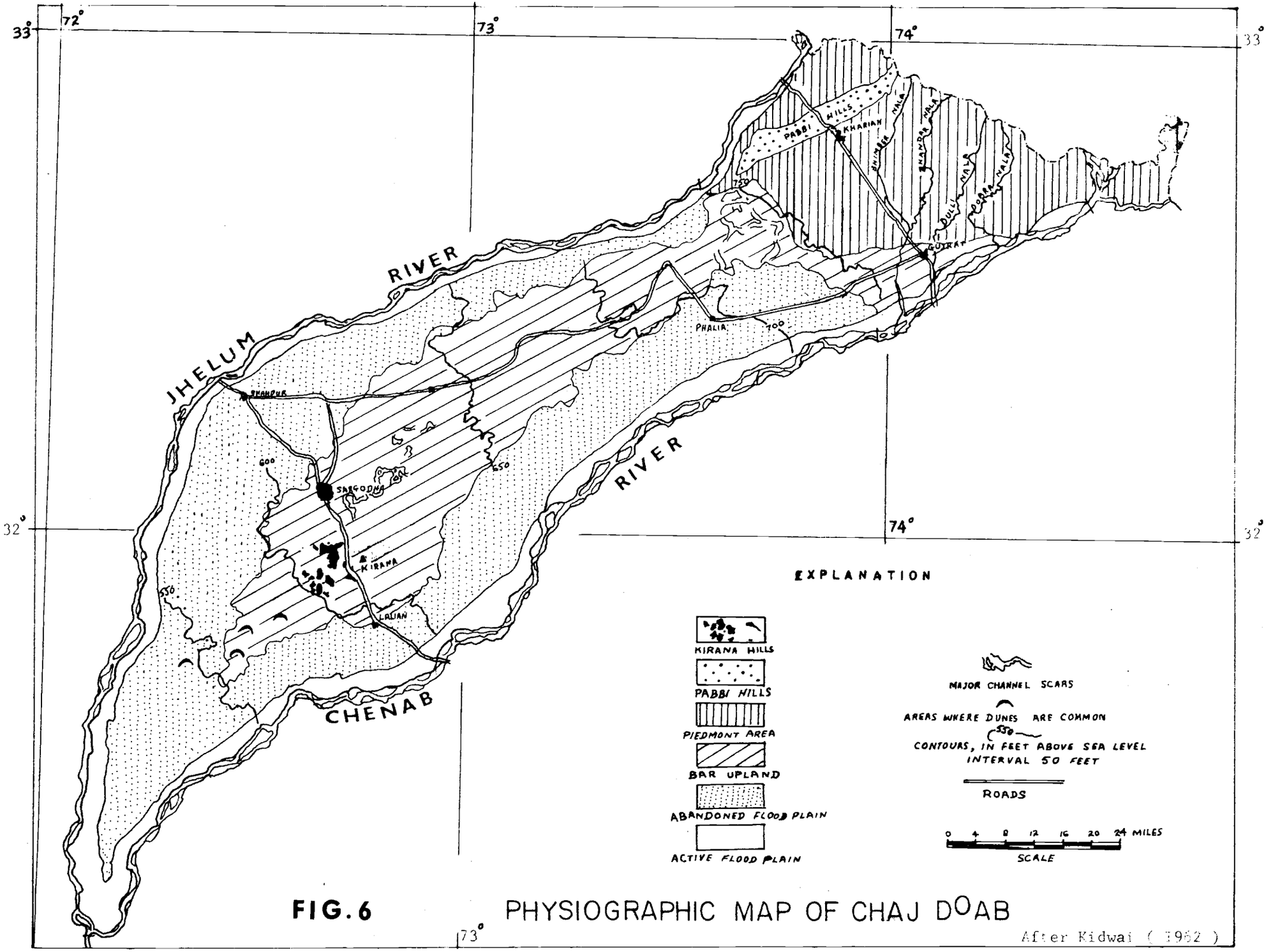

FIG. 6 PHYSIOGRAPHIC MAP OF CHAJ DOAB

After Kidwai (1962)

72° 73° 74°

32°

31°

JHELUM

SHAHPUR

SARGODHA

KIRANA

RIVER

CHENAB

RIVER

? ? ? ?

1200 1000 800 600 400

APPROXIMATE CONTOURS ON BEDROCK SURFACE, IN FEET BELOW LAND SURFACE

BEDROCK OUT—CROPS

8 6 4 2 0 4 8 12 16 MILES

SCALE

FIG.7 MAP SHOWING DEPTH TO BEDROCK IN CHAJ DOAB

AFTER KIDWAI 1962

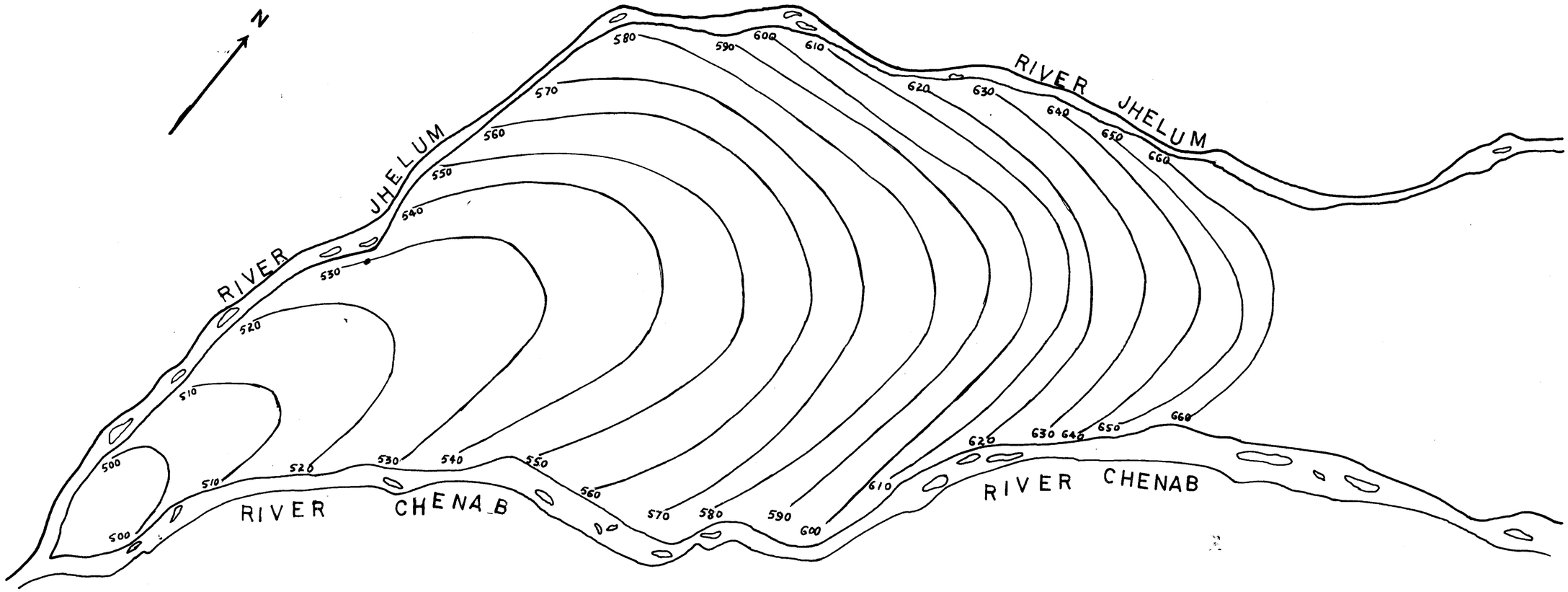

FIG. 10

GROUND WATER LEVEL CONTOURS (PRE-IRRIGATION)

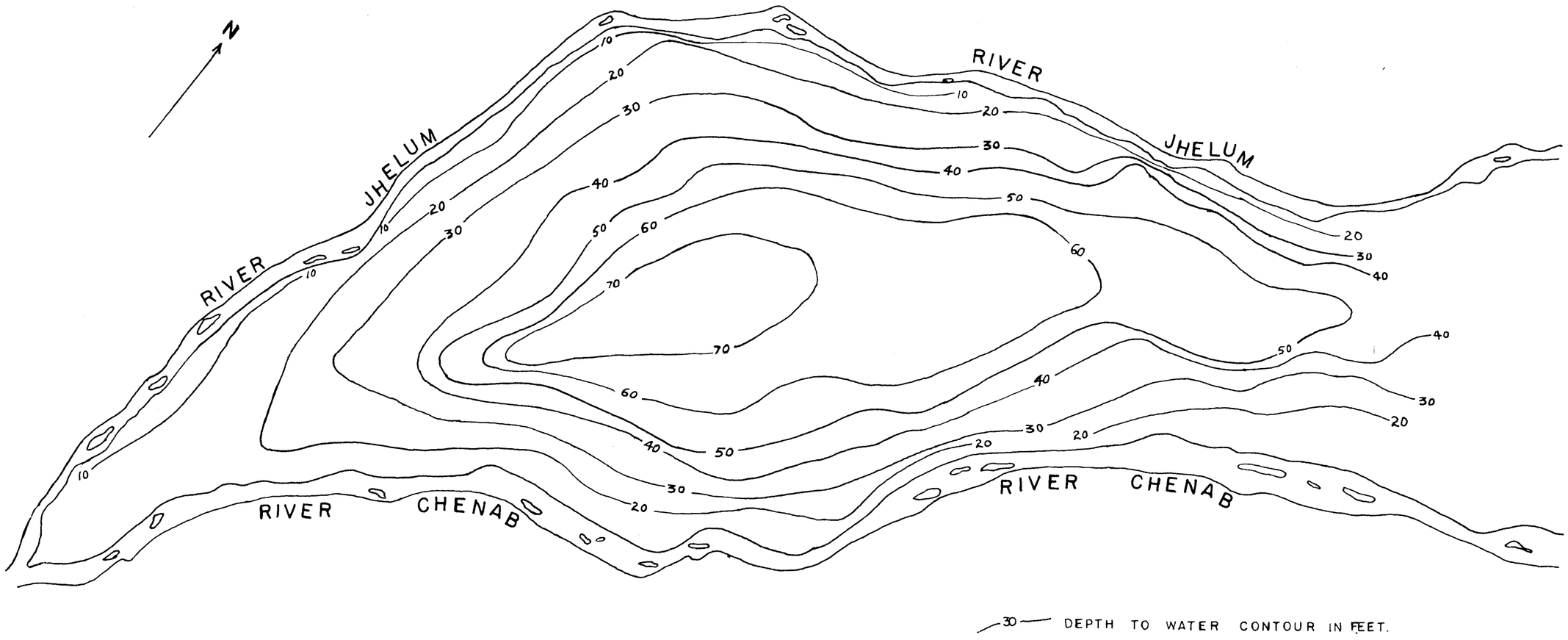

FIG. 11 MAP SHOWING DEPTH TO WATER BELOW LAND SURFACE (PRE-IRRIGATION PERIOD)

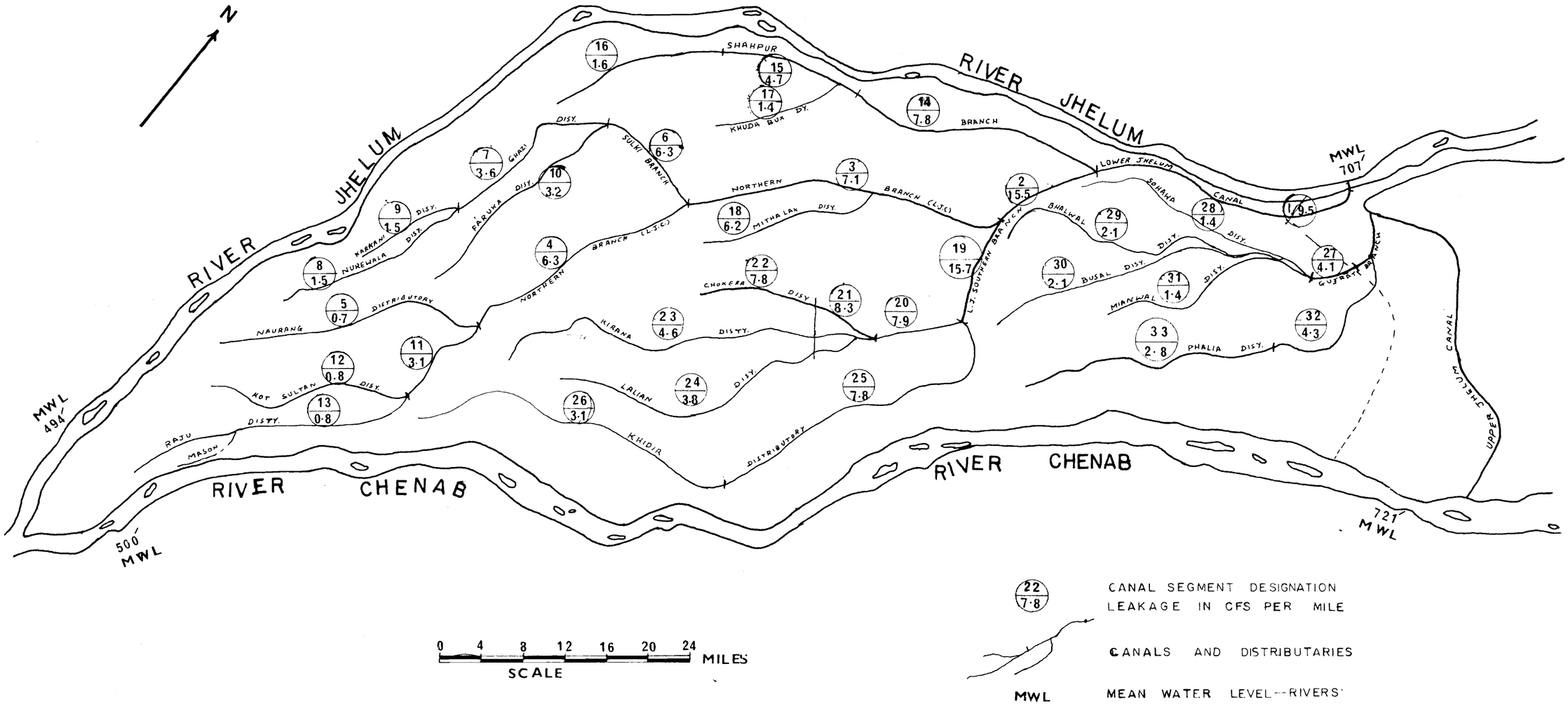

FIG. 12 MAP SHOWING LOCATION AND LEAKAGE FROM CANALS

ANALOG MODEL

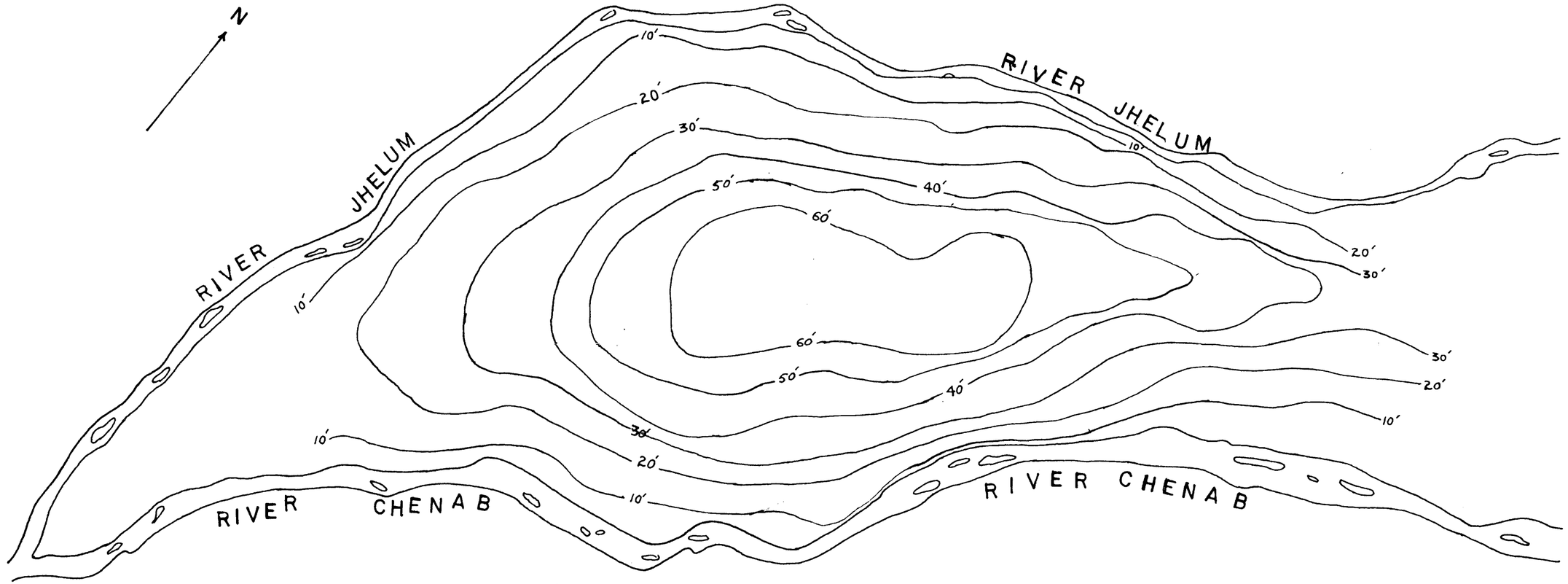

FIG. 13 CHANGE MAP SHOWING RISE IN GROUND WATER LEVELS (PRE-IRRIGATION TO 1960)

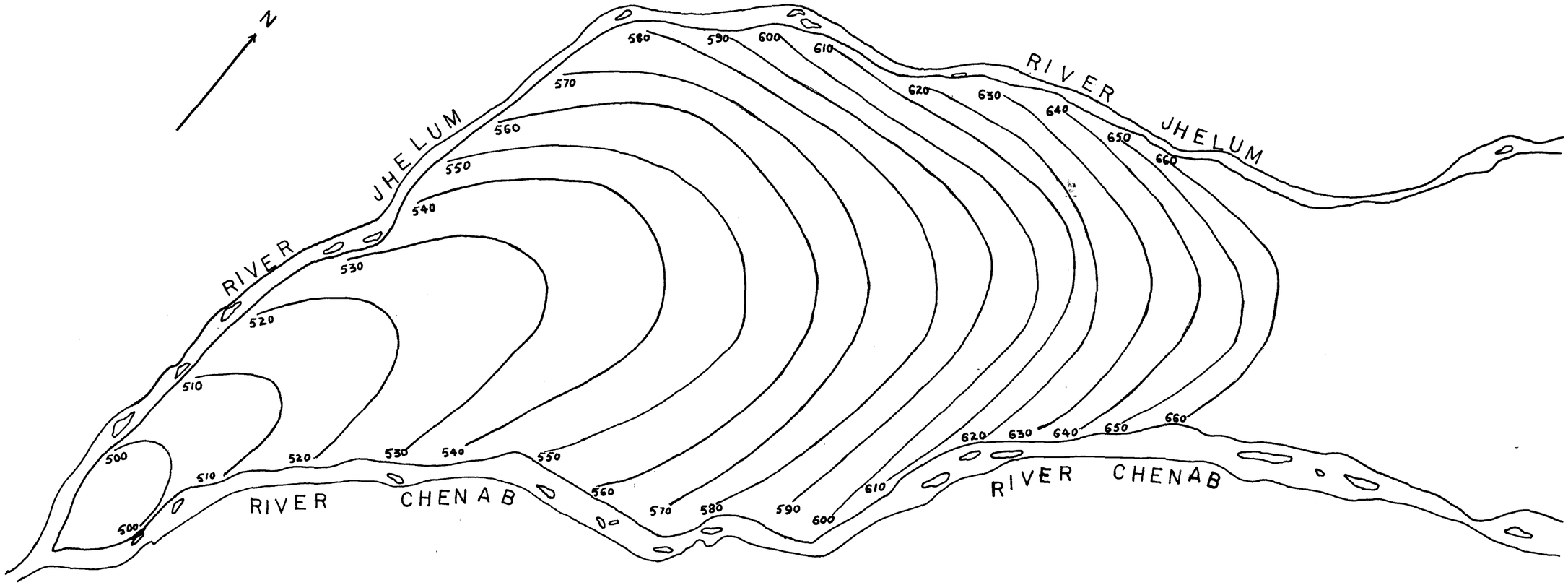

FIG. 16

GROUND WATER LEVEL CONTOURS (PRE-IRRIGATION)

ANALOG MODEL

59991
1964
92

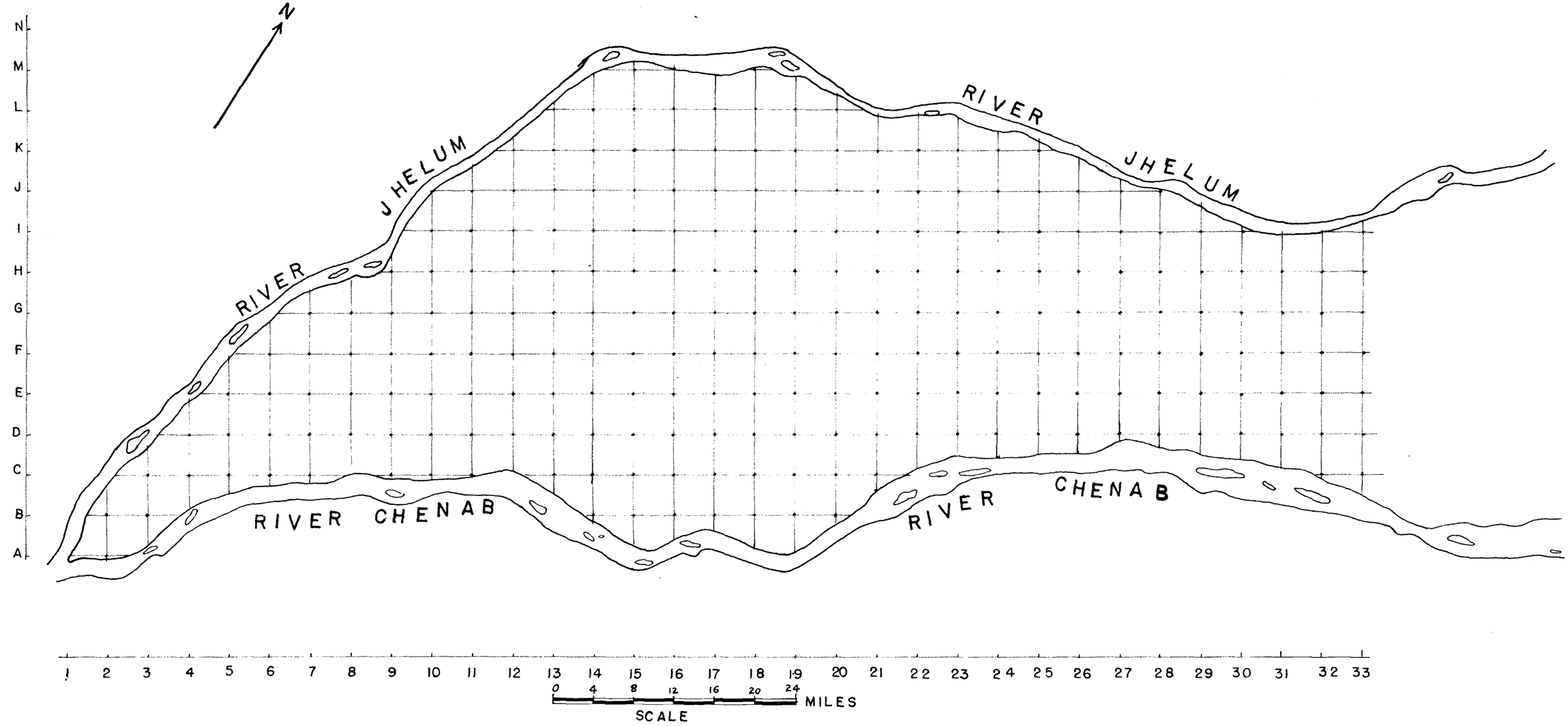

FIG. 17 MAP SHOWING CO-ORDINATES OF NODE-POINTS ON ANALOG MODEL NETWORK

E9791
1964
92

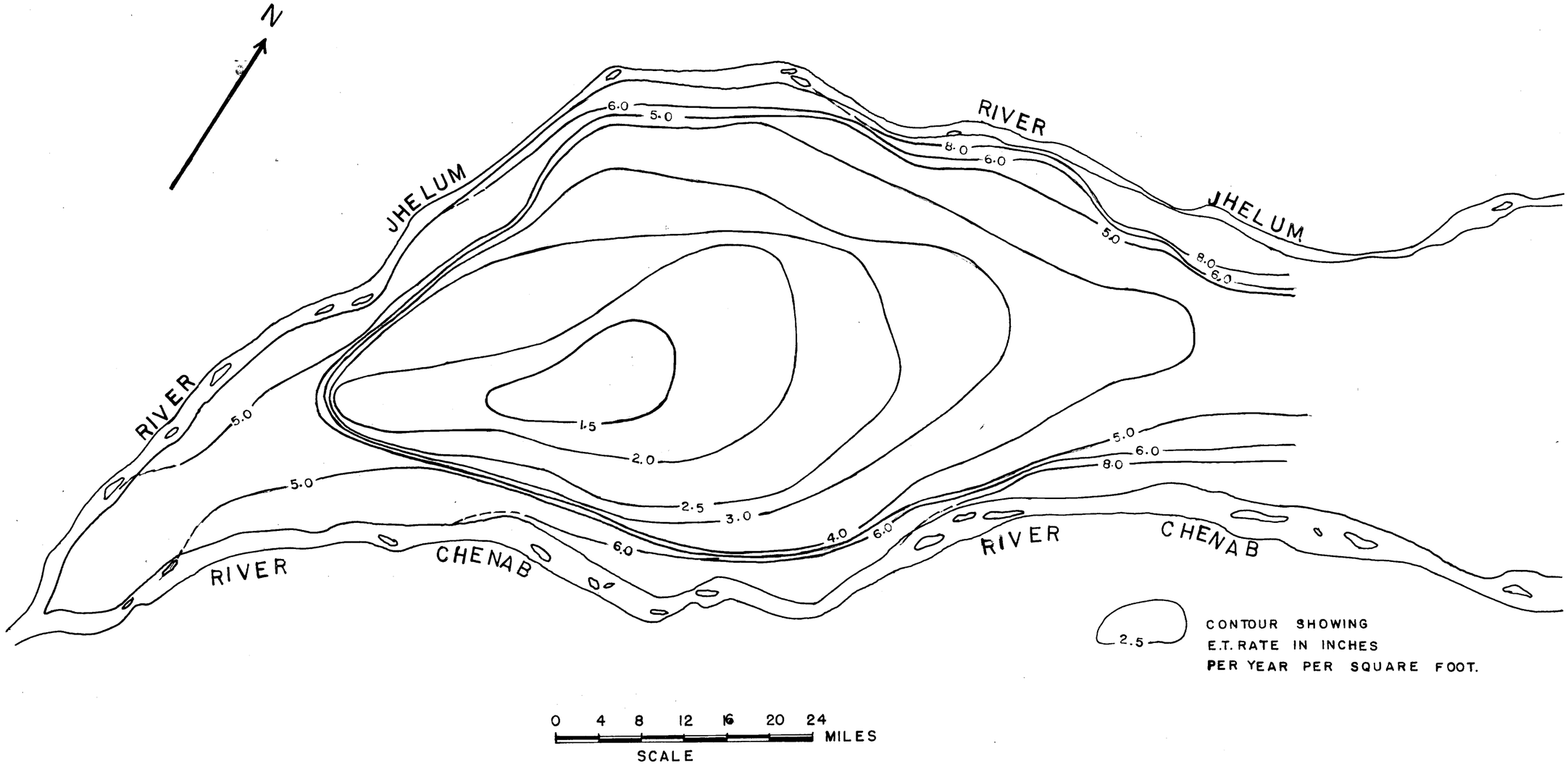

FIG. 18 MAP SHOWING EVAPOTRANSPIRATION OF PRE-IRRIGATION PERIOD (ANALOG MODEL)

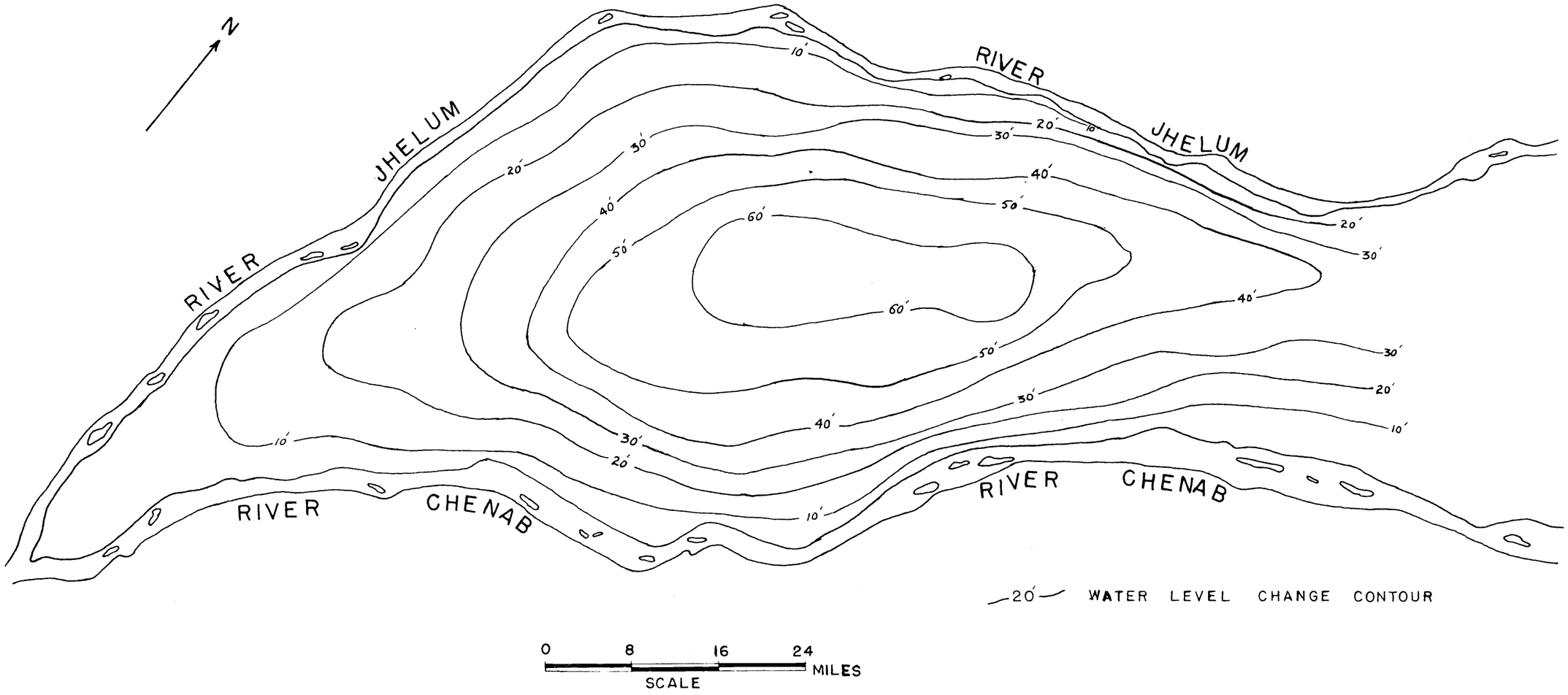

FIG.21 **CHANGE MAP SHOWING RISE IN GROUND WATER LEVELS (WITHOUT E.T.),** (PRE-IRRIGATION TO 1960)

ANALOG MODEL

E9791
1964
92

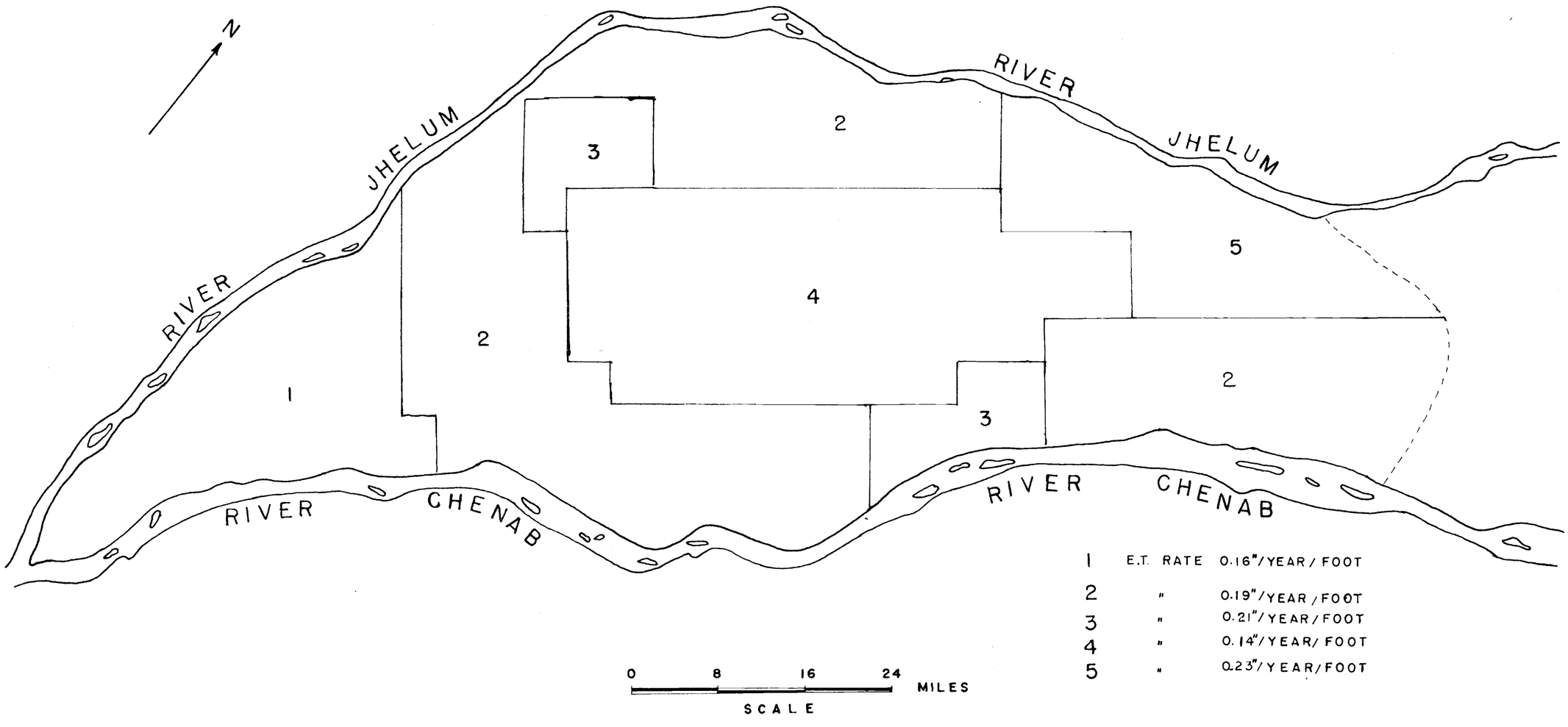

FIG. 23 MAP SHOWING ZONES OF EVAPOTRANSPIRATION RATE FOR NON-STEADY STATE ANALOG MODEL

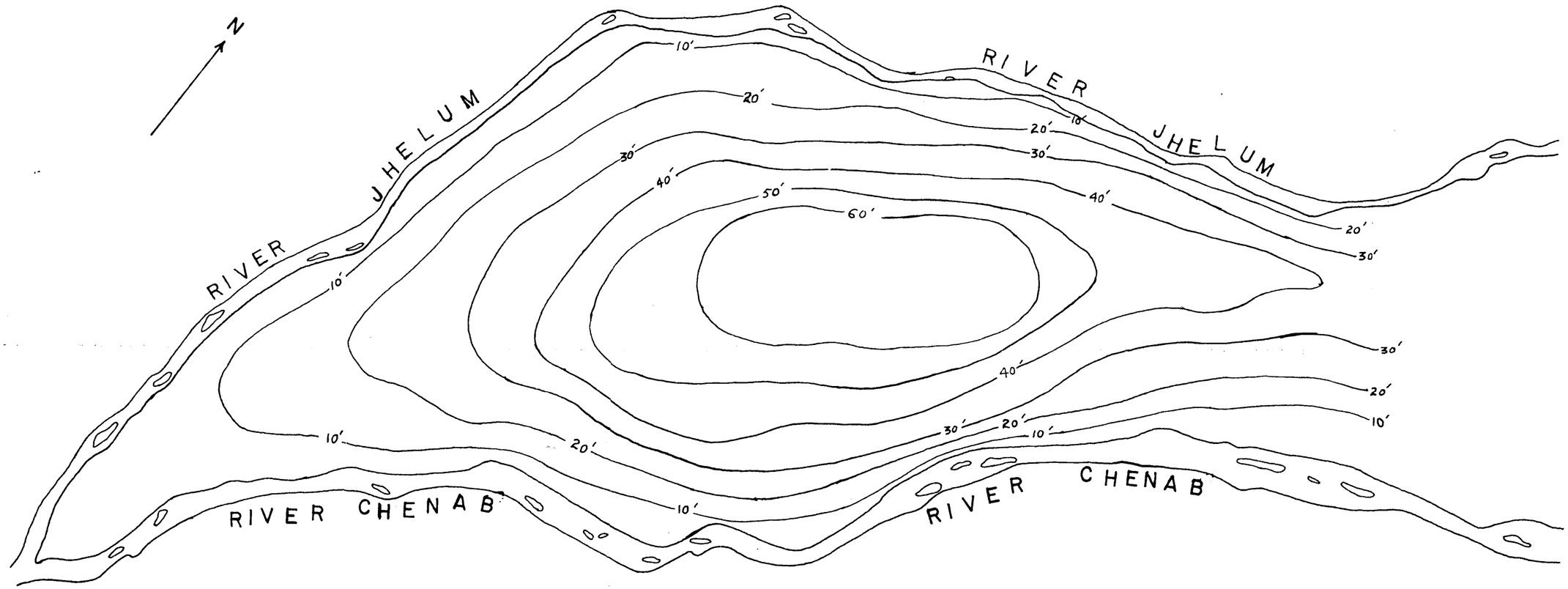

—20— WATER LEVEL CHANGE CONTOUR

0 8 16 24 MILES
SCALE

FIG.24 CHANGE MAP SHOWING RISE IN GROUND WATER LEVELS (WITH E.T.), (PRE IRRIGATION TO 1960).
ANALOG MODEL